

*We would like to sincerely thank Gabor for his feedback on the revision of our manuscript. We have responded to his remaining concerns as discussed in detail below and hope this sufficiently addresses his concerns before publication of the final version. We have highlighted his contributions more than the last version in the acknowledgements.*

Regarding the analyses of nucleus spectra, the inclusion of  $K(T)$  and  $k(T)$  is a clear improvement over the earlier version. As defined by the equations presented, these quantities provide absolute measures of INP concentration per volume of liquid (for rime and snow) and per volume of air (for the aerosol samples). However, a normalization is introduced (line 175) for reasons that are not clear. Perhaps it is done to compare the rime and snow samples with the aerosol samples on the same scale (line 314). That could be accomplished by plotting the two sets of data with different abscissa scales without the loss of absolute values of concentrations. As it is, the data from this paper cannot be compared to other results. Even on a procedural basis there is a problem: maximum values of  $k(T)$  are used as normalizing factor for each sample but these maximum values are obtained with very low values (usually 1 or 2) for both  $\Delta N$  and  $N(T)$  and so the ratio has large uncertainties and arbitrariness. The paper would gain from eliminating this normalization. If the authors insist on retaining it, the maximum values chosen should be presented.

*Thank you for highlighting this issue. We have removed the normalization from the spectra in all the figures so that absolute  $K(T)$  and  $k(T)$  can be assessed in comparison with reported values from other studies.*

Onset temperature and  $T_{10}$  and  $T_{50}$  are introduced as metrics for the INP measurements on lines 296-298 and are used in Fig. 6 (b) to (d) and in Section 3.3. This is understandable in view of the frequent use of these metrics in the past. Their use in this paper is regrettable as it goes against the goal stated in the title of the paper and elsewhere that spectra provide the focus of the analyses. The onset temperature is statistically a weak metric,  $T_{10}$  and  $T_{50}$  are somewhat better, but both are experiment specific, most significantly because of volume and sample size dependence. They do not constitute independent measures of activity to reinforce what is indicated by  $k(T)$  and  $K(T)$  and they are easily substituted by more defensible measures. In this paper, the value of  $K(T)$  at  $-15^{\circ}\text{C}$ ,  $K_{-15}$ , or at some other nearby temperature would be a good way to distinguish between results for different air-flow regimes. To re-state, the results shown in Fig. 6 (b) to (d) are not wrong, but by-pass the stated goal to use spectra measures and are weaker metrics than what the spectra could provide. Thus, the paper loses effectiveness. Comparisons to other works are hindered.

*We retain the use of onset temperature and  $T_{10}$  and  $T_{50}$  as the other goal was to assess the variability in INP spectra from the different directions from INCAS only, and meant not for quantitative comparison with previous measurements at Jungfraujoch or elsewhere. We have highlighted this goal in the second to last paragraph of the introduction to make this clear – that this is a secondary goal of the reported results.*

Why  $df/dT$  is retained in the analyses is somewhat puzzling. This quantity provides no information different from  $k(T)$  for the warm part of temperature range, i.e. for low values of  $f(T)$ , and is clearly an artifact at the cold end of the data range. As argued in my previous

comment (point #6)  $df/dT$  necessarily falls off when  $f(T)$  approaches unity and the location of the peak reflects primarily what fraction of the sample drops have already frozen at higher temperatures, not what is significant for the colder temperature region. Should the volume of the drops in the freezing tests been smaller, or should the water samples have been diluted with INP-free water, the  $df/dT$  peaks would have shifted to lower temperatures. As it is, the  $df/dT$  plots provide some comparison among the samples but are clearly misleading when used as a basis of interpreting the results in terms of INP types.

*The goal of showing  $df/dT$  is it clearly demonstrates modality between the samples from the different air mass directions when comparing samples within the current work. This metric has been used previously by Augustin et al. (2013) as stated on page 6 and has demonstrated utility in that one can compare the modal presence and height in the different temperature regimes. We regard this as a secondary but useful metric, thus, have retained it in the second revision but have made clear its limitations in section 3.2.*

Phrasing the results in terms of warm mode and cold mode INPs (lines 261-265 and more) is a tempting but imprecise argument. While peaks near  $-10^{\circ}\text{C}$  are significant, the cold mode is an artifact. The most common pattern of INP concentration functions is a monotonic increase toward colder temperatures. The monotonic increase can arise for a single material or for mixtures of several types of INPs. In general, the interpretation of signatures in  $k(T)$  is not yet well studied. When a peak is found in the differential spectra, the peak it can be assumed to represent either the presence of a specific INP material or a type of site configuration with frequency above the general trend. However, decomposing differential spectra in terms of different contributions will require much further work. The association of peaks near  $-10^{\circ}\text{C}$  with biological INP sources, and activity observed below about  $-17^{\circ}\text{C}$  with mineral sources should be made with more recognition of its tentative basis than is done in this manuscript. This is specially the case, since no independent analyses of composition, particle surface properties or other potentially relevant parameters are presented in this paper.

*Although we agree the cold mode is an artifact and experiment-specific, it provides insight into the different possible INP sources within the single INP sample population when using only to compare relative to the warm mode. The warm mode in  $df/dT$  is at the same temperature as in the differential spectra (as noted in the caption), and thus may be used for inter-sample comparison. Hence, we show the cold mode, but focus our discussion of sample comparison from the different air mass directions on the presence and location of the warm mode. The probability of the biological (warm mode) versus biological + mineral (cold mode) INPs is based on the current body of literature and is described on page 8. To emphasize the tentative basis of biological versus mineral INPs using spectra alone, we added the following sentence to section 3.2: "However, we note the tentative nature of characterizing these modes based on the previous body of literature and that more controlled, quantitative experiments of mixed biological-mineral INPs is needed in the future."*

Regarding different spectral features, it is remarkable that the slopes of the spectra below about  $-17^{\circ}\text{C}$  are very similar for the all snow and rime samples. While near  $-20^{\circ}\text{C}$  there is up to factor 100 range in concentration for the snow samples and not much less for the rime samples, the slopes are quite similar for all cases. Aerosol samples show more variability for the lower

temperature range but still aren't far from the trend seen in the snow and rime samples. Such features are noteworthy but the underlying causes are not yet clear.

*Interesting point! Perhaps something to evaluate in more detailed, control studies in the future.*

Minor points:

line 58: Seems like the word 'While' is an error

*'While' has been removed.*

line 67: 'intact' instead of 'in-tact'

*Done.*

line 80: 'intercomparison' doesn't express well the combined use of the data from the three different samples

*Changed to 'comparison'.*

lines 100-101: There is a substantial difference in how the main goals and accomplishments of the work are stated on lines 80-81 and on these lines.

*See response above. We have added the secondary goal of comparing INP spectra from the different air mass directions.*

line 109: 'inherent time' ???

*Removed 'inherent'.*

line 117: 'rime' instead of 'rimed'

*Done.*

line 117: What is known about the collection efficiency as a function of particle size for the intake configuration?

*While we have not conducted our own tests for collection efficiency, the DRUM has been intercompared and characterized by previous work (e.g., Cahill et al. (1987); although they used an 8-stage DRUM). Although the study by Bukowiecki et al. (2009) presents testing of collection efficiency tests with a different DRUM model as ours (i.e., they used a 3-stage DRUM), they demonstrate how rotating drum impactors are generally accurate and robust. We have added these references to section 2.1.*

*Bukowiecki, N., Richard, A., Furger, M., Weingartner, E., Aguirre, M., Huthwelker, T., Lienemann, P., Gehrig, R., and Baltensperger, U.: Deposition Uniformity and Particle*

*Size Distribution of Ambient Aerosol Collected with a Rotating Drum Impactor, Aerosol Sci Tech, 43, 891-901, 10.1080/02786820903002431, 2009.*

*Cahill, T. A., Feeney, P. J., and Eldred, R. A.: Size Time Composition Profile of Aerosols Using the Drum Sampler, Nucl Instrum Meth B, 22, 344-348, Doi 10.1016/0168-583x(87)90355-7, 1987.*

lines 145: The error introduced by variation in drop volume can be ascertained from the equations used for  $k(T)$  and  $K(T)$  -- it is of direct proportional magnitude. Stating this uncertainty as undetermined is incorrect.

*Removed 'undetermined'.*

line149: Was the variation in cooling rate due to slowing as the temperature lowered? Was it variable from one experiment to the other?

*The cold plate unfortunately does not have a uniform controllable cooling rate and typically slowed as the temperature was lowered and as the system reached its lower limit. It was variable from one experiment to the other, but only minorly variable (i.e., within uncertainty).*

line 162: 'average for each drop' ???

*Removed 'average'.*

lines 188, 195: Have BLI and SDE been defined?

*Yes, at the end of the introduction.*

line 331: 'not all samples contain a warm mode' would be better phrasing

*Done.*

line 350: This is a problem with the use of  $df/dT$  for analysis. If all drops froze at temperatures above about  $-17^{\circ}\text{C}$  for this sample, the concentration of less active nuclei could have been determined by dilution of the sample with nuclei-free water.

*This is true; however, we did not conduct dilution drop freezing testing thus cannot determine this with certainty. Still, the fact the warm mode was so dominant suggests that the warm temperature INPs were very abundant. For clarity, we did change this sentence to, "...indicating a relatively large contribution of warm temperature INPs as compared to the other samples from the study."*

line 371: 'differing' may be better instead of 'variable'

*Done.*

Fig. 6a: A legend placed inside the diagram area would be better than the one along the right-

side axis.

*Done.*

line 373: At what temperature is this range of concentrations evaluated?

*Over the entire spectrum (i.e., at all temperatures measured).*

# Using freezing spectra characteristics to identify ice nucleating particle populations during the winter in the Alps

Jessie M. Creamean<sup>1,2\*</sup>, Claudia Mignani<sup>3</sup>, Nicolas Bukowiecki<sup>4\*\*</sup>, Franz Conen<sup>3</sup>

<sup>1</sup>Cooperative Institute for Research in Environmental Sciences, University of Colorado, Boulder, CO, USA

<sup>2</sup>Physical Sciences Division, National Oceanic and Atmospheric Administration, Boulder, CO, USA

<sup>3</sup>Department of Environmental Sciences, University of Basel, Switzerland

<sup>4</sup>Laboratory of Atmospheric Chemistry, Paul Scherrer Institute, Villigen, Switzerland

\*Now at: Department of Atmospheric Science, Colorado State University, Fort Collins, CO, USA

\*\*Now at: 3

Email: jessie.creamean@colostate.edu

**Abstract.** One of the least understood cloud processes is modulation of their microphysics by aerosols, specifically of cloud ice by ice nucleating particles (INPs). To investigate INP impacts on cloud ice and subsequent precipitation formation, measurements in cloud environments are necessary but difficult given the logistical challenges associated with airborne measurements and separating interstitial aerosol from cloud residues. Additionally, determining the sources of INPs is important given the dependency of glaciation temperatures on the mineral or biological components and diversity of such INP populations. Here, we present results from a comparison of INP spectral characteristics in air, cloud rime, and fresh fallen snow at the High Altitude Research Station, Jungfraujoch. The goal of the study was two-fold: (1) to assess variability in wintertime INP populations found in-cloud based on wind and air mass direction during snowfall and (2) to evaluate possible INP sources between different sample types using a combination of cumulative INP ( $K(T)$ ), ~~normalized~~-differential fraction frozen ( $df/dT$ ), and ~~normalized~~-differential INP ( $k(T)$ ) spectra. INP freezing temperatures and concentrations were consistently higher on average from the southeast as compared to the northwest for rime, snow and especially aerosol samples which is likely a result of air mass influence from predominantly boundary layer terrestrial and marine sources in Southern Europe, the Mediterranean, and North Africa. For all three sample types combined, average onset freezing temperatures were  $-8.0$  and  $-11.3$  °C for southeasterly and northwesterly days, respectively, while  $K(T)$  were 3 to 20 times higher when winds arrived from the southeast. Southeasterly aerosol samples typically had a clear mode in the warm temperature regime (i.e.,  $\geq -15$  °C) in the  $df/dT$  and  $k(T)$  spectra—indicating a putative influence from biological sources—while the presence of a warm mode in the rime and snow varied. Evaluating  $df/dT$  concert with  $k(T)$  spectra exhibited variable modality and shape—depending on the types of INPs present—and may serve as a useful method for comparing different sampled substances and assessing the possible relative contributions of mixed mineral and biological versus only biological INP sample populations.

## 1 Introduction

Aerosols are key players in the atmospheric radiation budget, cloud microphysics, and precipitation development. Aerosol-induced ice microphysical modifications influence cloud lifetime and albedo (Albrecht, 1989; Twomey, 1977; Storelvmo et al., 2011), as well as the production of precipitation (DeMott et al., 2010). Mixed-phase clouds (MPCs) are ubiquitous in the troposphere over the entire annual cycle yet are difficult to quantify globally in part due to an inadequate understanding of aerosol-cloud interactions in mixed-phase environments (Korolev et al., 2017). Thus, a close evaluation of aerosol-cloud processes is crucial to evaluating weather and climate processes. However, one of the most significant challenges with regard to aerosols is quantifying their impacts on cloud ice formation through serving as ice nucleating particles (INPs) (Boucher et al., 2013). Constraining aerosol-cloud impacts

40 in models, specifically when parameterizing INPs in MPC systems, remains a significant challenge due to limited observations  
41 (Cziczo et al., 2017; Coluzza et al., 2017; DeMott et al., 2010; Kanji et al., 2017; Korolev et al., 2017). Observations directly in-  
42 cloud are even more scarce—given the logistical costs and resources required by airborne platforms, caveats associated with  
43 aircraft probes and instrumentation, and instrumental artefacts caused by flying through clouds at high speeds (Cziczo et al.,  
44 2017)—but are useful for assessing the impacts of INPs on MPC microphysics as compared to most surface measurements which  
45 are geared towards evaluation of INP sources.

46 In the absence of conditions with  $-38\text{ }^{\circ}\text{C}$  and relative humidity with respect to ice above 140%, INPs are required for initiation of  
47 tropospheric cloud ice formation (Kanji et al., 2017). Aerosols such as dust and primary biological aerosol particles (PBAPs) are  
48 some of the most abundant and efficient INPs found in the atmosphere, respectively (Murray et al., 2012; Hoose and Möhler, 2012;  
49 DeMott et al., 1999; Conen et al., 2011; Creamean et al., 2013). PBAPs originating from certain bacteria, pollens, and vegetative  
50 detritus are the most efficient INPs known, capable of initiating freezing near  $-1\text{ }^{\circ}\text{C}$ , while most PBAPs (e.g., fungal spores, algae,  
51 and diatoms) tend to nucleate ice at temperatures similar to those of mineral dust (Despres et al., 2012; Murray et al., 2012; Tobo  
52 et al., 2014; Hader et al., 2014a; O'Sullivan et al., 2014; Hill et al., 2016; Tesson et al., 2016; Alpert et al., 2011; Knopf et al., 2010;  
53 Fröhlich-Nowoisky et al., 2015). In general, previous works collectively indicate that PBAP INPs that nucleate ice at temperatures  
54 greater than approximately  $-10\text{ }^{\circ}\text{C}$  are bacterial (Murray et al., 2012; Hu et al., 2018; Hoose and Möhler, 2012; Despres et al.,  
55 2012; Fröhlich-Nowoisky et al., 2016), but could also be pollen or certain fungal spores (von Blohn et al., 2005; Hoose and Möhler,  
56 2012; O'Sullivan et al., 2016), although the latter two are less likely. Plant bacteria such as *Pseudomonas syringae* are deemed  
57 omnipresent in the atmosphere and precipitation (Despres et al., 2012; Stopelli et al., 2017; Morris et al., 2014), and facilitate cloud  
58 ice formation up to  $-1\text{ }^{\circ}\text{C}$  (Despres et al., 2012). ~~OW~~While, only a few laboratory-based studies have reported known inorganic or  
59 mineral materials with ice nucleation activity at such temperatures (Ganguly et al., 2018; Atkinson et al., 2013). Mineral and soil  
60 dust serving as atmospheric shuttles for organic microbial fragments can be transported thousands of kilometres and serve as  
61 effective INPs, even from highly arid regions such as the Sahara (Kellogg and Griffin, 2006). The origin of the ice nucleation germ  
62 forming at the warmest temperatures is thought to be due to the ice binding proteins or macromolecules of the biological  
63 components in mixed mineral-biological INPs (O'Sullivan et al., 2014; O'Sullivan et al., 2016; Conen and Yakutin, 2018). In  
64 general, the previous studies on the climate relevance of PBAPs demonstrate the importance of such INPs at MPC temperatures  
65 and precipitation enhancement (Morris et al., 2004; Bergeron, 1935; Christner et al., 2008; Morris et al., 2014; Morris et al., 2017;  
66 Stopelli et al., 2014; Fröhlich-Nowoisky et al., 2016).

67 Although biological constituents, from cellular material to in-tact bacteria and spores, are thought to be omnipresent in the  
68 atmosphere (Burrows et al., 2009b; Burrows et al., 2009a; Jaenicke, 2005; Jaenicke et al., 2007), modeling studies constraining  
69 global emission estimates of biological INPs and PBAPs are very limited, subject to significant hurdles, and often yield conflicting  
70 results due to not having a sufficient set of observations and complexity of atmospheric PBAPs (Hummel et al., 2015; Burrows et  
71 al., 2013; Twohy et al., 2016; Fröhlich-Nowoisky et al., 2012; Despres et al., 2012; Hoose and Möhler, 2012; Morris et al., 2011).  
72 Yet, biological aerosols such as bacteria have been shown to cause significant perturbations in cloud ice in numerical weather  
73 prediction models, affording modulations in cloud radiative forcing and precipitation formation (Sahyoun et al., 2017). In addition,  
74 measuring and quantifying PBAPs is non-trivial—methodologies for counting, culturing, and nucleic acid sequencing of PBAPs  
75 and especially for those which fall in the warm temperature INP regime (i.e., INPs that nucleate ice  $> -15\text{ }^{\circ}\text{C}$ ) are: (1) time and  
76 labor intensive, (2) require specific expertise or at times substantial resources, (3) require substantial sample volumes, or (4) are  
77 species- or genera-specific or limited to viable microorganisms (Despres et al., 2012). Although such techniques are required to

78 adequately assess the atmospheric microbiome and PBAP sources, a simpler approach could be applied to evaluate and even  
79 quantify warm temperature biological INP populations as compared to colder temperature PBAPs or mineral dust.

80 The objectives of the study presented here are: (1) to conduct an ~~inter~~comparison of INP measurements of aerosol, cloud rime, and  
81 snow directly in-cloud and (2) evaluate different types of INP spectra in a manner such that we can estimate the relative contribution  
82 from biological INPs in the warm temperature regime relevant to MPCs. A secondary goal is to assess the variability in INP spectra  
83 and possible sources from different dominant air mass transport directions observed during sample collection under the current  
84 study. Sampling was conducted at the High Altitude Research Station Jungfraujoch (JFJ), a unique location for evaluating  
85 populations of INPs that affect winter storms in the European Alps, and where MPCs are particularly common (Lohmann et al.,  
86 2016). Recent studies at JFJ have provided valuable insight into INP concentrations, sources, and removal processes under a variety  
87 of conditions and during various times of the year. Conen et al. (2015) measured INPs at  $-8^{\circ}\text{C}$  over the course of a year at JFJ,  
88 and found a strong seasonality in such INPs, with two order of magnitude higher concentrations observed during the summer. They  
89 also suggested INPs measured at this temperature may be limited most of the year by microphysical processing during transit.  
90 Stopelli et al. (2015) verified this removal mechanistic process through INP measurements and isotopic composition of fresh fallen  
91 snow at JFJ, concluding that warm temperature INPs are rapidly depleted by precipitating clouds at lower elevations. Stopelli et  
92 al. (2016) expanded their INP analyses to 2-years of data at JFJ, concluding that a high abundance of INPs at  $-8^{\circ}\text{C}$  is to be expected  
93 whenever high wind speed coincides with air masses having experienced little or no precipitation prior to sampling, yet a separate  
94 study by Stopelli et al. (2017) found that only a small fraction of the INPs were cultivable cells of *Pseudomonas syringe*. In contrast,  
95 Lacher et al. (2018a; 2018b) conducted an interannual synopsis of INP measurements at JFJ and found anthropogenic influence  
96 on INP concentrations but only during boundary layer intrusion (BLI) and at relatively cold temperatures (i.e., approximately  $-30$   
97  $^{\circ}\text{C}$ ), and higher INP concentrations during Saharan dust events (SDEs) and marine boundary layer air arriving at JFJ. Eriksen  
98 Hammer et al. (2018) characterized ice particle residuals and concluded that silica and aluminosilicates were the most important  
99 ice particle residuals at JFJ during the mixed-phase cloud events during Jan – Feb 2017, while carbon-rich particles of possible  
100 biological origin were a minor contribution.

101 Here, we demonstrate how variable sources influence INP populations depending on air mass transport and direction, and spectral  
102 modality between the rime, snow, and aerosols can help explain the exchange of INPs from air into cloud then into precipitation.  
103 Our results expand upon previous studies by evaluating INPs via a combination of aerosol, rime, and snow, and at a temperature  
104 range that comprises common biological and mineral INPs.

## 105 **2 Methods**

### 106 **2.1 Aerosol, cloud rime and snow collection at Jungfraujoch**

107 Collocated collection of snow, cloud rime, and aerosol samples for the Ice Nucleation Characterization in the Alps of Switzerland  
108 (INCAS) study took place 15 Feb – 11 Mar 2018 in the Sphinx observatory at JFJ ( $46.55^{\circ}\text{N}$ ,  $7.98^{\circ}\text{E}$ ; 3580 m above sea level (m  
109 a.s.l.); <https://www.hfsjg.ch/en/home/>). Snow was collected as described by Stopelli et al. (2015) using a Teflon-coated tin (0.1  
110  $\text{m}^2$ , 8 cm deep) for a duration of 1 – 18 hours, but typically for 1 – 4 hours. Collection quantities and ~~inherent~~-time of collection  
111 were dependent upon snowfall rates but additionally on winds blowing snow out of the collection pans. Because of this possibility,  
112 we cannot determine actual snowfall rates with certainty. Cloud rime was collected using a slotted plexiglass plate placed vertically  
113 during snow sample collection (Lacher et al., 2017; Mignani et al., 2018). Sample collection times were at times longer than the  
114 duration of in-cloud conditions (see section 2.3) and were dependent on when manually changing the sampling tin and plate was

115 possible. Daily size-resolved aerosol samples were collected using a Davis Rotating-drum Universal-size-cut Monitoring (DRUM)  
116 single-jet impactor (DA400, DRUMAir, LLC.) (Cahill et al., 1987; Bukowiecki et al., 2009; Creamean et al., 2018a) from a 1-m  
117 long inlet constructed of 6.4-mm inner diameter static-dissipative polyurethane tubing (McMaster-Carr®) leading to outside of the  
118 Sphinx and connected to a funnel covered with a loose, perforated plastic bag to prevent rime~~d~~ ice build-up or blowing snow from  
119 clogging the inlet. The DRUM collected aerosol particles at four size ranges (0.15 – 0.34, 0.34 – 1.20, 1.20 – 2.96, and 2.96 – >12  
120  $\mu\text{m}$  in diameter) and sampled at 27.7 L  $\text{min}^{-1}$  (volumetric flow), equalling 39888 total L of air per sample. Such size ranges cover  
121 a wide array of aerosols—particularly those that serve as INPs (DeMott et al., 2010; Fridlind et al., 2012; Mason et al.,  
122 2016)—while the large volume of air collected promotes collection of rarer, warm temperature biological INPs, but may represent  
123 a lower fraction of overall INP concentrations (Mossop and Thorndike, 1966). Samples were deposited onto 20 x 190 mm strips  
124 of petrolatum-coated (100%, Vaseline®) perfluoroalkoxy plastic (PFA, 0.05 mm thick) substrate secured onto the rotating drums  
125 (20 mm thick, 60 mm in diameter) in each of the four stages at the rate of 7 mm per day (5 mm of sample streaked onto the PFA  
126 followed by 2 mm of blank). It is possible local sources of aerosol, such as tobacco smoke or emissions from touristic infrastructure,  
127 were collected by the DRUM (Bukowiecki et al., 2016), but did not likely affect the 2.96 – >12  $\mu\text{m}$  particles which we focus on  
128 herein. Intervals in which snow, rime, and aerosol were sampled did not fully overlap during a day because conditions were  
129 changing often unpredictably between out-of-cloud and in-cloud conditions, the latter with or without precipitation. At the same  
130 time we intended to collect enough material from either component for a robust analysis of warm temperature INPs. Consequently,  
131 the combined data of a day integrate over a larger air mass, including clouds and cloud-free regions. Comparing data from snow,  
132 rime, and aerosol samples still makes sense as long as wind direction and the influence of planetary boundary layer did not change  
133 substantially during a day.

## 134 **2.2 Ice nucleation measurements**

135 All samples were analysed immediately after collection for INPs using a drop freezing cold plate system described by Creamean  
136 et al. (2018b; 2018a). Briefly, snow and cloud rime samples were melted into covered 50-mL glass beakers for analysis, resulting  
137 in approximately 10 mL of liquid per sample. Samples were manually shaken prior to analysis. Aerosols deposited onto the PFA  
138 were prepared for drop freezing by cutting out each daily sample and placing in a 50-mL glass beaker with 2 mL of molecular  
139 biology reagent grade water (Sigma-Aldrich®). Beakers were covered and shaken at 500 rpm for 2 hours (Bowers et al., 2009). In  
140 between sampling, beakers were cleaned with isopropanol (99.5%), sonicated with double-distilled water for 30 minutes, and then  
141 heated at 150 °C for 30 minutes.

142 Copper discs (76 mm in diameter, 3.2 mm thick) were prepared by sonicating in double-distilled water for 30 minutes, cleaning  
143 with isopropanol, then coated with a thin layer of petrolatum (Tobo, 2016; Bowers et al., 2009). Following sample preparation, a  
144 sterile, single-use syringe was used to draw 0.25 mL of the suspension and 100 drops were pipetted onto the petrolatum-coated  
145 copper disc, creating an array of ~2.5- $\mu\text{L}$  aliquots. Drops were visually inspected for size; however, it is possible not all drops were  
146 the same exact volume, which could lead to a small level of ~~undetermined~~-uncertainty (Hader et al., 2014b; Bigg, 1953; Langham  
147 and Mason, 1958; Creamean et al., 2018b). The copper disc was then placed on a thermoelectric cold plate (Aldrich®) and covered  
148 with a transparent plastic dome. Small holes in the side of the dome and copper disc permitted placement of up to four temperature  
149 probes using an Omega™ thermometer/data logger (RDXL4SD; 0.1 °C resolution and accuracy of  $\pm (0.4\% + 1\text{ }^\circ\text{C})$  for the K sensor  
150 types used). During the test, the cold plate was cooled at 1 – 10 °C  $\text{min}^{-1}$  from room temperature until around –35 °C. Control  
151 experiments at various cooling rates within this range show very little discernible dependency of drop freezing on cooling rate  
152 (Creamean et al., 2018b), akin to previous works (Wright and Petters, 2013; Vali and Stansbury, 1966).

153 A +0.33 °C correction factor was added to any temperature herein and an uncertainty of 0.15 °C was added to the probe accuracy  
 154 uncertainty based on DFCP characterization testing presented in Creamean et al. (2018b), to account for the temperature difference  
 155 between the measurement (i.e., in the plate centre) and actual drop temperature. Frozen drops were detected visually but recorded  
 156 through custom software. The software records the time, probe temperature, and cooling rate for every second of the test. When a  
 157 drop is identified as frozen, a button is clicked on the software graphical user interface so that it records that exact time, probe  
 158 temperature, and cooling rate of that drop in a separate file. The test continued until all 100 drops were frozen. Each sample was  
 159 tested three times with 100 new drops for each test. The fraction frozen was calculated from all detected drops frozen combined  
 160 from the three tests (typically, > 90% of the drops were detected). The results from the triplicate tests were then binned every 0.5  
 161 °C to produce one spectrum per sample. Cumulative INP concentrations were calculated using the equation from Vali (1971):

$$162 \quad K(T) = -\frac{1}{V_{drop}} \times \ln[1 - f(T)]$$

163 Where  $V_{drop}$  is the ~~average~~ volume of each drop and  $f(T)$  is the fraction of drops frozen at temperature  $T$ . ~~Normalized d~~Differentials  
 164 of the frequency of freezing events, or  $df/dT$ , were calculated finding the difference in  $f(T)$  at each temperature bin of 0.5 °C ~~and~~  
 165 ~~normalizing to the maximum  $df/dT$  value per sample~~, then smoothed using a moving average. Aerosol cumulative INP  
 166 concentrations were corrected for the total volume of air per sample ( $K(T) \times \frac{V_{suspension}}{V_{air}}$ ) while melted rime/snow residual  
 167 cumulative INPs were adjusted to the total used during analysis ( $K(T) \times V_{suspension}$ ), where  $V_{suspension}$  and  $V_{air}$  represent the total  
 168 liquid volume analyzed per sample (0.75 mL for the three tests) and total volume of air drawn per sample (39888 L), respectively.

169 Differential INP spectra—which as the name indicates, correspond to the differential of the cumulative spectra (Vali et al., 2015)—  
 170 were used early in earlier studies (Vali, 1971; Vali and Stansbury, 1966). Spectra from these previous studies only reached a  
 171 minimum of −20 °C due to the limitations of background artifacts in the water used at that time. Recent work by Vali (2018) revisits  
 172 the use of differential spectra, expanding to lower temperatures. We employ the calculation for differential INP concentrations  
 173 from Vali (2018):

$$174 \quad k(T) = -\frac{1}{V_{drop} \times \Delta T} \times \ln\left(1 - \frac{\Delta N}{N(T)}\right)$$

175 where  $N$  is the number of unfrozen drops and  $\Delta N$  is the number of freezing events observed between  $T$  and  $(T - \Delta T)$ . Differential  
 176 concentrations were divided by the maximum concentration per sample (i.e., to normalize) then smoothed using a moving average.

### 177 **2.3 Supporting meteorological and source analysis data**

178 Auxiliary surface meteorological observations, including but not limited to hourly mean air temperature measured 2 m above  
 179 ground level (a.g.l.) (°C), relative humidity measured 2 m a.g.l. (%), scalar wind speed ( $\text{m s}^{-1}$ ) and direction (degrees), and incoming  
 180 longwave radiation ( $\text{W m}^{-2}$ ) were acquired from MeteoSwiss (<https://gate.meteoswiss.ch/idaweb/>). From the longwave  
 181 measurements, in-cloud conditions were determined by calculating the sky temperature and comparing to air temperature measured  
 182 at the station, per the methodology of Herrmann et al. (2015) from a 6-year analysis of JFJ observations. There were no in situ  
 183 measurements of cloud presence or extent. For the current work, each hourly measurement was categorized as out-of-cloud or in-  
 184 cloud based on such calculations and averaged to obtain daily cloud coverage percentage.

185 Radon ( $^{222}\text{Rn}$ ) concentrations have been continuously measured at JFJ since 2009. Details on the detectors themselves and the  
186 measurements can be found in Griffiths et al. (2014). Briefly, 30-minute radon concentrations were measured using a dual-flow-  
187 loop two-filter radon detector as described by Chambers et al. (2016). Calibrated radon concentrations were converted from activity  
188 concentration at ambient conditions to a quantity which is conserved during an air parcel's ascent: activity concentration at standard  
189 temperature and pressure (0 °C, 1013 hPa), written as  $\text{Bq m}^{-3}$  STP (Griffiths et al., 2014). Time periods with BLI were classified  
190 as radon concentrations  $> 2 \text{ Bq m}^{-3}$  (Griffiths et al., 2014). Particle concentrations from approximately 0.3 to  $> 20 \mu\text{m}$  in diameter  
191 were measured with a 15-channel optical particle sizer (OPS 3300; TSI, Inc.) at a 1-minute time resolution (Bukowiecki et al.,  
192 2016). Due to operational complications, OPS data were not collected prior to 23 Feb during INCAS. Air was drawn through a  
193 heated total aerosol inlet (25 °C) which, besides aerosol particles, enables hydrometeors with diameters  $< 40 \mu\text{m}$  to enter and to  
194 evaporate, at wind speeds of  $20 \text{ m s}^{-1}$  (Weingartner et al., 1999). SDEs were determined from existing methodology using various  
195 aerosol optical properties, but specifically, the Ångström exponent of the single scattering albedo ( $\hat{a}_{\text{SSA}}$ ), which decreases with  
196 wavelength during SDEs (Collaud Coen et al., 2004; Bukowiecki et al., 2016). SDEs are automatically detected by the occurrence  
197 of negative  $\hat{a}_{\text{SSA}}$  that last more than four hours. Based on previous work, most of the SDEs do not lead to a detectable increase of  
198 the 48-h total suspended particulate matter concentrations at JFJ (Collaud Coen et al., 2004). Additionally, we consider these events  
199 probable SDEs, but may have influences from other sources in addition.

200 Air mass transport analyses were conducted using the HYbrid Single Particle Lagrangian Integrated Trajectory model with the  
201 SplitR package for RStudio (<https://github.com/rich-iannone/SplitR>) (Draxler, 1999; Draxler and Rolph, 2011; Stein et al., 2015).  
202 Reanalysis data from the National Centers for Environmental Prediction (NCEP) National Center for Atmospheric Research  
203 (NCAR) (2.5° latitude-longitude; 6-hourly; [https://www.ready.noaa.gov/gbl\\_reanalysis.php](https://www.ready.noaa.gov/gbl_reanalysis.php)) were used as the meteorological fields  
204 in HYSPLIT simulations. Air mass transport directionality and frontal passages were verified by NCEP/NCAR reanalyses of wind  
205 vectors and geopotential height at 600 mb (i.e., approximate pressure at the altitude of JFJ;  
206 <https://www.esrl.noaa.gov/psd/data/composites/day/>). Trajectories were initiated at 10, 500, and 1000 m a.g.l. every 3 hours daily,  
207 but only the 500-m trajectories are shown. Trajectories were only simulated for each northwesterly, southeasterly, SDE, and BLI  
208 case study day (i.e., Table 1). It is important to note that “northwesterly” is a contribution of north, west, and northwest winds,  
209 while “southeasterly” includes south, east, and southeast winds. SDE and BLI days were predominantly (not entirely) southeasterly.

## 210 **3 Results and discussion**

### 211 **3.1 Directional dichotomy of air masses arriving at JFJ during INCAS**

212 Local surface meteorology was variable at JFJ during INCAS, with air temperatures ranging from  $-27.5$  to  $-4.8$  °C (average of  $-$   
213  $13.7$  °C)—temperatures relevant to heterogeneous nucleation of cloud ice—and relative humidity ranging from 18 to 100% (Figure  
214 1a). All days contained some fraction of in-cloud conditions that varied between 12% and 100%, on average. Due to the topography  
215 surrounding JFJ, predominant wind directions were northwest followed by southeast, with the fastest winds recorded originating  
216 from the southeast (Figure 2). Such conditions are typical for JFJ during the winter (Stopelli et al., 2015; Collaud Coen et al.,  
217 2011). Out of the entire study, several days were classified as northwesterly (5 days) or southeasterly (2 days) conditions when a  
218 combination of aerosol, cloud rime, and snow samples were collected (i.e., a full 24 hours of northwesterly or a full 24 hours of  
219 southeasterly winds during snowfall; Table 1), which are herein focused on as the case study days (indicated by the blue and red  
220 in Figure 1b, respectively). These days were also deemed days with “storm” conditions since clouds and snow were both present  
221 at JFJ. There were 4 days that maintained predominantly southerly wind directions as indicated in green in Figure 1b and Table 1

222 and were characterized as days influenced by SDEs or BLI as discussed herein. Rime and snow were only collected on one of these  
223 days, while remaining SDE or BLI cases had only aerosol collected. Aside from 22 Feb (missing data), the remaining days in the  
224 study were characterized as FT and did not exhibit influences from warm temperature INPs (see section 3.2 and 3.3).

225 Most southeasterly case days (and 06 Mar) apart from the SDE days experienced longer residence times in what was likely the  
226 boundary layer (i.e., 1000 m or less) compared to northwesterly cases, which is supported by radon data (Figure 1c). Griffiths et  
227 al. (2014) determined that radon concentrations  $> 2 \text{ Bq m}^{-3}$  signify BLI, which in the current work was clearly observed on 23 Feb,  
228 27 Feb, 28 Feb, 06 Mar, and 11 Mar case days, indicating samples collected on these days were likely influenced by continental  
229 boundary layer sources. Relatively low radon concentrations were observed the remaining case study days, indicating these samples  
230 were predominantly affected by free tropospheric (FT) air and thus, lower aerosol concentrations and/or more distant, including  
231 marine, sources. Although OPS data were missing until 23 Feb, source information can be gleaned from the available data. For  
232 example, 23 Feb had episodic high concentrations of particles (maximum of  $9.6 \text{ cm}^{-3}$ ) towards the beginning of the day coincident  
233 with the largest spike in radon, with a steady decrease as time transpired, indicating the boundary layer was an ample source of  $>$   
234  $0.3 \mu\text{m}$  particles. A similar episode with the OPS and radon concentrations was observed 27 – 28 Feb, where the highest  
235 concentrations of each were observed during the entire study period. Selected days were subject to diurnal winds (not shown), such  
236 as 06 Mar, where boundary layer air reached JFJ and a midday maximum in OPS particle concentrations was observed, indicating  
237 lower elevations were the dominant source of aerosol. Although, diurnal variations in aerosol from local sources have been shown  
238 to not be common in the winter at JFJ (Baltensperger et al., 1997). In contrast, 11 Mar was exposed to boundary layer air based on  
239 radon observations, but particle concentrations were low (average of  $0.2 \text{ cm}^{-3}$  compared to a study average of  $3.0 \text{ cm}^{-3}$ ), signifying  
240 that although BLI occurred at JFJ, it was not a substantial source of aerosol. These relationships corroborate the ice nucleation  
241 observations, as discussed in detail below.

242 Extending past local conditions, air mass transport 10 days back in time prior to reaching JFJ on case study days was, as expected,  
243 dissimilar between northwesterly (Figure 3) and southeasterly/SDE/BLI (Figure 4) conditions. The main distinctions between  
244 northwesterly and southeasterly/SDE/BLI days are: (1) northwesterly days originated from farther west, with some days reaching  
245 back to North America, while air masses on southeasterly/SDE/BLI days predominantly hovered over land and oceanic sources  
246 closer to Europe, (2) southeasterly/SDE/BLI air masses travelled closer to the surface relative to northwesterly days, while  
247 northwesterly air masses were typically transported from higher altitudes (i.e., more FT exposure), and (3) aside from 6 Mar (which  
248 is discussed in more detail in the following section), northwesterly air masses did not travel over the Mediterranean and northern  
249 Africa, whereas the southeasterly/SDE/BLI air masses above JFJ arrived from over such regions within less than 2 days before  
250 arriving to JFJ. One obvious inconsistency is that the air mass trajectories on 24 Feb do not indicate transport occurred from  
251 Northern Africa even though this day was characterized as an SDE. Collaud Coen et al. (2004) reported that in 71% of all cases  
252 they evaluated at JFJ, 10-day back-trajectories were able to reveal the source of Saharan dust and that back trajectories cannot  
253 always explain SDEs. Boose et al. (2016) reported similar transport pathways for JFJ during multiple consecutive winters and  
254 concluded that marine and Saharan dust served as dominant sources of INPs at  $-33 \text{ }^\circ\text{C}$ . Reche et al. (2018) also reported similar  
255 pathways and sources for bacteria and viruses, but during the summer in southern Spain. These disparate sources and transport  
256 pathways of air support the variability in the ice nucleation observations as discussed in more detail in the following section.

### 257 **3.2 Variability in INP spectra based on air mass source**

258 Out of the 25 aerosol, 30 rime, and 39 snow samples collected, 7 aerosol, 19 rime, and 23 snow were collected northwesterly or  
259 southeasterly storm case study days, while 4 aerosol, 1 rime, and 2 snow were collected on SDE or BLI days (Table 1). Most mixed

260 wind direction days were excluded, as sources from both directions would contribute to the daily aerosol sample. Figure 5 shows  
261 the cumulative ( $K(T)$ ) INP concentrations, ~~normalized~~-differential fraction frozen per 0.5 °C temperature interval ( $df/dT$ ), and  
262 ~~normalized~~-differential ( $k(T)$ ) INP concentrations from aerosol, snow, and rime samples on the case days. The use of  $df/dT$  is  
263 limited in that it is while qualitative and ~~possibly~~-method-specific in terms of modality locations, but demonstrates the presence of  
264 1 – 2 INP populations by having a mode in the warm regime (i.e., warm mode or likely ~~primarily~~-biological) and/or cold regime  
265 (i.e., < 15 °C; cold mode or likely a mixture of mineral and biological) (Augustin et al., 2013) and enables us to intercompare  
266 between the different types of samples from different air mass sources at JFJ.

267 In addition to containing higher concentrations of warm temperature INPs, most southeasterly and SDE/BLI samples contained a  
268 clear mode in the warm temperature regime compared to northwesterly samples which typically did not contain such a mode in  
269 the  $df/dT$  and  $k(T)$  spectra. This warm mode, or “bump” at temperatures above approximately –15 °C has been observed in a wide  
270 range of previous immersion mode ice nucleation studies including but not limited to some of the earliest studies of total aerosol  
271 (Vali, 1971), residuals found in hail (Vali and Stansbury, 1966), sea spray aerosol (McCluskey et al., 2017; DeMott et al., 2016),  
272 soil samples (Hill et al., 2016), agricultural harvesting emissions (Suski et al., 2018), and in recent reviews of aerosol (Kanji et al.,  
273 2017; DeMott et al., 2018) and precipitation (Petters and Wright, 2015) samples. Most previous studies that show spectra with the  
274 warm mode typically: (1) report a wide range of freezing temperatures such that it can be observed relative to the steady increase  
275 of INPs at colder temperatures or (2) are of samples that include a mixture of biological and mineral or other less efficient INP  
276 sources. For example, several previous studies report INP concentrations down to only –15 °C (e.g., Conen and Yakutin, 2018;  
277 Hara et al., 2016; Kieft, 1988; Schnell and Vali, 1976; Vali et al., 1976; Wex et al., 2015), namely because the goal was to target  
278 efficient, warm-temperature biological INPs. However, the warm mode may not be evident in such studies, given it cannot be  
279 visualised next to the drastic increase in INPs with temperatures below –15 °C (i.e., the cold mode). In contrast, studies conducting  
280 INP measurements on known mineral dust samples also are not able to observe the warm mode (e.g., Price et al., 2018; Atkinson  
281 et al., 2013; Murray et al., 2012). Together, it is apparent that a mixed biological and mineral (or less efficient biological INPs)  
282 sample is needed to assess the modal behaviour in the INP spectra. However, we note the tentative nature of characterizing these  
283 modes based on the previous body of literature and that more controlled, quantitative experiments of mixed biological-mineral  
284 INPs is needed in the future.

285 Only the largest size range of the aerosol is shown because the remaining size ranges (i.e., < 2.96 µm) were not distinct with respect  
286 to wind direction. The fact that size, alone, exhibited directionally-dependent results and that such dependencies were only  
287 observed in the coarse mode aerosol indicate: (1) the sources were indeed different between northwesterly, southeasterly, and  
288 SDE/BLI transport—supporting the air mass source analyses—and (2) the coarse mode aerosols were likely from a regional source  
289 as opposed to long-range transported thousands of kilometres. This is because gravitational settling typically renders transport of  
290 coarse particles inefficient especially within the boundary layer (Creamean et al., 2018a; Jaenicke, 1980). Previous work by Collaud  
291 Coen et al. (2018) concludes that the local boundary layer infrequently influences JFJ in the winter, supporting the current work  
292 (i.e., more FT days (17 of 25 days); Table 1).

293 Generally, INPs from southeasterly and SDE/BLI days were higher in concentration and more efficient (i.e., were warm  
294 temperature INPs that facilitated ice formation > –15 °C) than northwesterly samples. Our results are parallel to those by Stopelli  
295 et al. (2016), who also observed higher  $K(T)$  in snow samples collected during southerly conditions at JFJ from Dec 2012 to Oct  
296 2014 (Figure 6a). However,  $K(T)$  reported here were generally higher than those reported by Stopelli et al. (2016), especially for

297 the northwesterly samples. Unlike Stopelli et al. (2016), there was no clear correlation between  $K(T)$  with air temperature and wind  
298 speed in the current work (not shown).

299 Onset freezing temperatures (i.e., the highest temperature in which the first drop in each sample froze) were typically higher for  
300 southeast/SDE/BLI samples as compared to the northwest (Figure 6b), indicating influences from sources that produce warm  
301 temperature INPs on these days. The temperatures in which 10% ( $T_{10}$ ) and 50% ( $T_{50}$ ) of the samples froze were also typically  
302 higher for the southeast/SDE/BLI as compared to the northwest samples, especially for the aerosol samples, indicating higher  
303 concentrations of more efficient warm temperature INPs.

304 Regarding the snow, it is possible that surface processes generate airborne ice particles, which contribute to a snow sample collected  
305 at a mountain station (Beck et al., 2018). However, snow that is re-suspended during a snowfall event largely consists of the most  
306 recently fallen snow crystals covering wind-exposed surfaces. These particles are unlikely to be different from concurrently falling  
307 snow. Hence, their contribution will not change INP abundance or spectral properties of the collected sample. Another matter are  
308 hoar frost crystals, which can be very abundant in terms of number, but because of their small size (i.e.,  $< 100 \mu\text{m}$  (Lloyd et al.,  
309 2015)) can only make a minor contribution to the mass of solid precipitation depositing in a tin placed horizontally on a mountain  
310 crest. The majority of small crystals will follow the streamlines of air passing over the crest. All that an increased influence of hoar  
311 frost particles would do to our observations is to decrease measured differences between snow and rime samples, because additions  
312 of hoar frost, a form of rime, would render the collected snow sample a bit more similar to rime.

### 313 **3.3 Potential components of INP populations at JFJ**

314 Taking the spectral characteristics in the context of air mass direction and transport can help elucidate the possible sources of INPs  
315 at JFJ during INCAS. Qualitative and quantitative evaluation of the warm mode, or likely, the relative contribution of warm  
316 temperature biological INPs, to cold mode INPs is transparent when  $df/dT$  and  $k(T)$  are calculated (Figure 6e – g). Additionally,  
317 normalizing such spectra affords a qualitative comparison of spectra signatures between aerosols and residuals found in cloud rime  
318 and snow. We offer some possible explanations for the observed variability between the samples. Naturally, the boundary layer  
319 more frequently than not contains higher concentrations of warm temperature INPs—and INPs in general—as compared to the  
320 free troposphere given the proximity to the sources (e.g., forests, agriculture, vegetation, and the oceans) (Burrows et al., 2013;  
321 Despres et al., 2012; Frohlich-Nowoisky et al., 2016; Wilson et al., 2015; Burrows et al., 2009a; Burrows et al., 2009b; Frohlich-  
322 Nowoisky et al., 2012; Suski et al., 2018). Although, microorganisms and nanoscale biological fragments are episodically lofted  
323 into the free troposphere with mineral dust and transported thousands of kilometres (Creamean et al., 2013; Kellogg and Griffin,  
324 2006).

325 Air arriving at JFJ on 15 and 16 Feb originated from the farthest away and were not heavily exposed to boundary layer air, as  
326 evidenced by the air mass trajectory analysis (Figure 3) and radon (Figure 1c), indicating long-range transport in the free  
327 troposphere. This could explain why the warm mode (and higher  $T_{10}$  and  $T_{50}$ ) was observed for the rime and snow, but not the  
328 aerosol—the aerosol had sufficient time to nucleate ice during free tropospheric transport and especially the warm temperature  
329 INPs that would likely become depleted in-cloud first (Stopelli et al., 2015), assuming the clouds formed along the air mass  
330 transport pathways. Cloud fraction was relatively low (12.5 to 25%), but air temperatures were relatively high ( $-8.4$  to  $-7.1$  °C),  
331 suggesting conditions were amenable for long-range transported warm temperature INPs to nucleate cloud ice. However, from the  
332 available data, we cannot determine with certainty if the local conditions were the same as those when nucleation initially occurred.  
333 For 19 and 20 Feb, air temperature was cold ( $-16.4$  and  $-19.6$  °C, respectively) cloud fraction was high (92 and 54%, respectively),

334 and ~~all samples did not contain a warm mode~~not all samples contained a warm mode. One possible explanation is that any warm  
335 temperature INPs that were present in the clouds had already snowed out prior to reaching the sampling location, as observed by  
336 Stopelli et al. (2015) at JFJ. Although, given the low radon concentrations and erratic transport pathways, it is possible such air  
337 masses did not contain a relatively large concentrations of warm temperature INPs due to deficient exchange with the boundary  
338 layer. It was not until the southeasterly cases that the aerosol samples exhibited a warm mode. Specifically, on 23 Feb local winds  
339 shifted to southeasterly (147 degrees on average) and air masses arrived from over the eastern Alps, Eastern Europe, Scandinavia,  
340 and earlier on in time, the Atlantic Ocean. Thus, these samples were predominantly influenced by the continental (mostly over  
341 remote regions) and marine boundary layers, where sources of warm temperature INPs are more abundant (Frohlich-Nowoisky et  
342 al., 2016).

343 The northwesterly case of 06 Mar is somewhat interesting in that the local wind direction was clearly from the northwest, but air  
344 mass source analyses show brief transport in the boundary layer (radon) from the south, when looking farther back in time, traveling  
345 over the Mediterranean and North Africa. The aerosol sample had a high onset temperature for INPs relative to other northwest  
346 samples (Figure 6b) and snow samples exhibited a warm mode (Figure 6g). It is the only one of the northwesterly case samples  
347 that encountered boundary layer exposure according to the radon observations. Combined, these results suggest a somewhat mixed-  
348 source sample, and that 06 Mar may not be directly parallel to the other northwesterly cases. Transitioning back to a southeasterly  
349 case on 11 Mar, only the rime and snow unveiled a warm mode from air transported from similar regions as the 06 Mar sample.  
350 Additionally, OPS concentrations were very low (Figure 1c). These results suggest the aerosols already nucleated cloud ice prior  
351 to reaching JFJ on 11 Mar (i.e., low ambient aerosol), where the aerosol did not contain a warm mode, but rime and snow did.

352 When evaluating the SDE and BLI days, there is a bit of variability. On 24 Feb, clouds were present at JFJ (a cloud fraction of  
353 37.5%), but riming was insufficient to collect enough quantity for INP analysis and no snowfall occurred. Interestingly, the warm  
354 mode was the second highest for the aerosol sample and it did not contain a cold mode (for  $df/dT$ ), indicating a relatively large  
355 contribution of warm temperature INPs as ~~compared to the total INP population~~compared to the other samples from the study. Air  
356 mass transport was very similar to 23 Feb signifying similar INP sources even though this day was characterized as an SDE, but it  
357 is probable that a slightly warmer ( $-6.0$  as compared to  $-9.8$  °C air temperature), drier (79 versus 89% relative humidity), and  
358 higher pressure (649 versus 645 mb) postfrontal system moved over JFJ on 24 Feb, inhibiting removal of warm temperature INPs  
359 during transport relative to the day prior (corroborated by reanalysis from NCEP/NCAR of geopotential height at 600 mb). The  
360 BLI case of 28 Feb was very similar to 24 Feb in that: (1) only an aerosol sample was collected and (2) the warm mode was the  
361 maximum mode for  $df/dT$ . As compared to 27 Feb where a warm mode was not observed, 28 Feb was warmer ( $-20.0$  as compared  
362 to  $-26.2$  °C), drier (52 versus 62%), higher pressure (635 versus 630 mb), and had a warmer onset temperature ( $-6.8$  versus  $-14.8$   
363 °C). Wind direction was slightly different: southeasterly (153 degrees) on 27 Feb as compared to southwesterly on 28 Feb (221  
364 degrees). However, conditions were cloudier than the 23 – 24 Feb coupling and completely cloudy on 27 Feb (100 and 66.7%  
365 cloud fraction on 27 Feb and 28 Feb, respectively). Additionally, radon and OPS concentrations were the highest on 27 – 28 Feb  
366 as compared to the rest of the days during INCAS (Figure 1c). Combined, these results suggest a very local, boundary layer source  
367 of INPs started on 27 Feb, but were quickly depleted in the very cloudy conditions. Once clouds started to clear and a shift in  
368 frontal characteristics occurred, a similar source of very efficient warm temperature INPs affected JFJ but were able to be observed  
369 in the aerosol.

#### 370 **4 Conclusions and broader implications**

371 Aerosol, cloud rime, and snow samples were collected at the High Altitude Research Station Jungfrauoch during the INCAS field  
372 campaign in Feb and Mar 2018. The objectives of the study were to assess variability in wintertime INP sources found in cloudy  
373 environments and evaluate relationships between INPs found in the different sample materials. To directly compare air to liquid  
374 samples, characteristics of ~~normalized~~-differential fraction frozen and INP spectra were compared in the context of cumulative INP  
375 spectra statistics, air mass transport and exposure to boundary layer or free tropospheric conditions, and local meteorology.  
376 Distinction between northwesterly and southeasterly conditions yielded ~~variable-differing~~ results regarding INP efficiency and  
377 concentrations, biological versus non-biological sources, and meteorological conditions at the sampling location. In general,  
378 cumulative INP concentrations were 3 to 20 times higher for all sample types when sources from the southeast infiltrated JFJ,  
379 while the INP spectra of the aerosol contained a warm mode but the presence of a warm mode was variable for the rime and snow  
380 depending on meteorological context.

381 In general, comprehensive measurements of INPs from aerosol, and rime and snow when possible, affords useful information to  
382 compare and explain exchange between aerosols, clouds, and precipitation in the context of local and regional scale meteorology  
383 and transport conditions. Assessment of different INP spectral types, modality, and spectra statistics adds another dimension for  
384 qualitative and semi-quantitative intercomparison of sampling days and evaluation of associations between aerosol, cloud, and  
385 precipitation sampling. Extending INP analyses past reporting cumulative concentrations affords more detailed information on the  
386 population of INPs and enables comparison between samples from aerosols, clouds, precipitation, and beyond (e.g., seawater, soil,  
387 etc.). Using auxiliary measurements and air mass simulations, in addition to context provided by previous work at JFJ, we have  
388 addressed possible sources for INCAS. However, more detailed source apportionment work should be imminent to  
389 comprehensively characterize INP sources based on spectral features. Future studies should ideally use such statistical analyses in  
390 tandem with focused chemical and biological characterization assessments to provide direct linkages between INP spectral  
391 properties and sources. Such investigations could yield valuable information on INP sources, and aerosol-cloud-precipitation  
392 interactions, which could then be used to improve process-level model parameterizations of such interactions by rendering  
393 quantitative information on INP source, efficiency, and abundance. Improving understanding of aerosol impacts on clouds and  
394 precipitation will ultimately significantly enhance understanding of the earth system with respect to cloud effects on the surface  
395 energy and water budgets to address future concerns of climate change and water availability.

#### 396 **Author contributions**

397 JMC collected the samples, conducted the DFA sample analysis, conducted data analysis, and wrote the manuscript. CM and FC  
398 also contributed to collecting rime and snow samples. JMC, CM, and FC designed the experiments. NB provided quality controlled  
399 OPS data. CM, NB, and FC helped with manuscript feedback and revision prior to submission.

#### 400 **Acknowledgements**

401 The Swiss National Science Foundation (SNF) financially supported JMC within its Scientific Exchanges Programme, through  
402 grant number IZSEZO\_179151. The work of CM and FC on Jungfrauoch is made possible through SNF grant number  
403 200021\_169620. Radon measurements were performed as part of the Swiss contribution to ICOS ([www.icos-ri.eu](http://www.icos-ri.eu)). Aerosol data  
404 were acquired by Paul Scherrer Institute in the framework of the Global Atmosphere Watch (GAW) programme funded by  
405 MeteoSwiss. We would like to thank Gabor Vali, one other anonymous reviewer, and Martin Gysel for their valuable feedback

406 during the review process. Specifically, we would like to acknowledge and highlight Gabor Vali's contributions that provoked  
407 significant improvement of the manuscript during the review process. Further support was received from the ACTRIS2 project  
408 funded through the EU H2020-INFRAIA-2014-2015 programme (grant agreement no. 654109) and the Swiss State Secretariat for  
409 Education, Research and Innovation (SERI; contract number 15.0159-1). The opinions expressed and arguments employed herein  
410 do not necessarily reflect the official views of the Swiss Government. We are grateful to the International Foundation High Altitude  
411 Research Stations Jungfrauoch and Gornergrat (HFSJG), 3012 Bern, Switzerland, for providing through its infrastructure  
412 comfortable access to mixed-phase clouds. Special thanks go to Joan and Martin Fischer, and Christine and Ruedi Käser, the  
413 custodians of the station. The authors gratefully acknowledge the NOAA Air Resources Laboratory (ARL) for the provision of the  
414 HYSPLIT transport and dispersion model and/or READY website (<http://www.ready.noaa.gov>) used in this publication.

## 415 References

- 416 Albrecht, B. A.: Aerosols, Cloud Microphysics, and Fractional Cloudiness, *Science*, 245, 1227-1230,  
417 10.1126/science.245.4923.1227, 1989.
- 418 Alpert, P. A., Aller, J. Y., and Knopf, D. A.: Ice nucleation from aqueous NaCl droplets with and without marine diatoms, *Atmos.*  
419 *Chem. Phys.*, 11, 5539-5555, 10.5194/acp-11-5539-2011, 2011.
- 420 Atkinson, J. D., Murray, B. J., Woodhouse, M. T., Whale, T. F., Baustian, K. J., Carslaw, K. S., Dobbie, S., O'Sullivan, D., and  
421 Malkin, T. L.: The importance of feldspar for ice nucleation by mineral dust in mixed-phase clouds, *Nature*, 498, 355-  
422 358, 10.1038/nature12278, 2013.
- 423 Augustin, S., Wex, H., Niedermeier, D., Pummer, B., Grothe, H., Hartmann, S., Tomsche, L., Clauss, T., Voigtländer, J., Ignatius,  
424 K., and Stratmann, F.: Immersion freezing of birch pollen washing water, *Atmos. Chem. Phys.*, 13, 10989-11003,  
425 10.5194/acp-13-10989-2013, 2013.
- 426 Baltensperger, U., Gäggeler, H. W., Jost, D. T., Lugauer, M., Schwikowski, M., Weingartner, E., and Seibert, P.: Aerosol  
427 climatology at the high-alpine site Jungfrauoch, Switzerland, *Journal of Geophysical Research: Atmospheres*, 102,  
428 19707-19715, doi:10.1029/97JD00928, 1997.
- 429 Beck, A., Henneberger, J., Fugal, J. P., David, R. O., Lacher, L., and Lohmann, U.: Impact of surface and near-surface processes  
430 on ice crystal concentrations measured at mountain-top research stations, *Atmos Chem Phys*, 18, 8909-8927, 10.5194/acp-  
431 18-8909-2018, 2018.
- 432 Bergeron, T.: On the physics of cloud and precipitation, 5th Assembly of the U.G.G.I., Paul Dupont, Paris, 1935.
- 433 Bigg, E. K.: The Supercooling of Water, *P Phys Soc Lond B*, 66, 688-694, Doi 10.1088/0370-1301/66/8/309, 1953.
- 434 Boose, Y., Sierau, B., Garcia, M. I., Rodriguez, S., Alastuey, A., Linke, C., Schnaiter, M., Kupiszewski, P., Kanji, Z. A., and  
435 Lohmann, U.: Ice nucleating particles in the Saharan Air Layer, *Atmos. Chem. Phys.*, 16, 9067-9087, 2016.
- 436 Boucher, O., Randall, D., Artaxo, P., Bretherton, C., Feingold, G., Forster, P., Kerminen, V.-M., Kondo, Y., Liao, H., Lohmann,  
437 U., Rasch, P., Satheesh, S. K., Sherwood, S., Stevens, B., and Zhang, X. Y.: Clouds and Aerosols, in: *Climate Change*  
438 *2013: The Physical Science Basis. Contribution of Working Group I to the Fifth Assessment Report of the*  
439 *Intergovernmental Panel on Climate Change*, edited by: Stocker, T. F., Qin, D., Plattner, G.-K., Tignor, M., Allen, S. K.,  
440 Boschung, J., Nauels, A., Xia, Y., Bex, V., and Midgley, P. M., Cambridge University Press, Cambridge, United Kingdom  
441 and New York, NY, USA, 571-658, 2013.
- 442 Bowers, R. M., Lauber, C. L., Wiedinmyer, C., Hamady, M., Hallar, A. G., Fall, R., Knight, R., and Fierer, N.: Characterization  
443 of Airborne Microbial Communities at a High-Elevation Site and Their Potential To Act as Atmospheric Ice Nuclei,  
444 *Applied and Environmental Microbiology*, 75, 5121-5130, 10.1128/Aem.00447-09, 2009.
- 445 Bukowiecki, N., Richard, A., Furger, M., Weingartner, E., Aguirre, M., Huthwelker, T., Lienemann, P., Gehrig, R., and  
446 Baltensperger, U.: Deposition Uniformity and Particle Size Distribution of Ambient Aerosol Collected with a Rotating  
447 Drum Impactor, *Aerosol Science and Technology*, 43, 891-901, 10.1080/02786820903002431, 2009.
- 448 Bukowiecki, N., Weingartner, E., Gysel, M., Coen, M. C., Zieger, P., Herrmann, E., Steinbacher, M., Gäggeler, H. W., and  
449 Baltensperger, U.: A Review of More than 20 Years of Aerosol Observation at the High Altitude Research Station  
450 Jungfrauoch, Switzerland (3580 m asl), *Aerosol and Air Quality Research*, 16, 764-788, 10.4209/aaqr.2015.05.0305,  
451 2016.
- 452 Burrows, S. M., Butler, T., Jockel, P., Tost, H., Kerkweg, A., Poschl, U., and Lawrence, M. G.: Bacteria in the global atmosphere  
453 - Part 2: Modeling of emissions and transport between different ecosystems, *Atmos Chem Phys*, 9, 9281-9297, DOI  
454 10.5194/acp-9-9281-2009, 2009a.
- 455 Burrows, S. M., Elbert, W., Lawrence, M. G., and Poschl, U.: Bacteria in the global atmosphere - Part 1: Review and synthesis of  
456 literature data for different ecosystems, *Atmos Chem Phys*, 9, 9263-9280, DOI 10.5194/acp-9-9263-2009, 2009b.
- 457 Burrows, S. M., Hoose, C., Poschl, U., and Lawrence, M. G.: Ice nuclei in marine air: biogenic particles or dust?, *Atmos Chem*  
458 *Phys*, 13, 245-267, 10.5194/acp-13-245-2013, 2013.

459 Cahill, T. A., Feeney, P. J., and Eldred, R. A.: Size Time Composition Profile of Aerosols Using the Drum Sampler, *Nucl Instrum*  
460 *Meth B*, 22, 344-348, Doi 10.1016/0168-583x(87)90355-7, 1987.

461 Chambers, S. D., Williams, A. G., Conen, F., Griffiths, A. D., Reimann, S., Steinbacher, M., Krummel, P. B., Steele, L. P., van  
462 der Schoot, M. V., Galbally, I. E., Molloy, S. B., and Barnes, J. E.: Towards a Universal "Baseline" Characterisation of  
463 Air Masses for High- and Low-Altitude Observing Stations Using Radon-222, *Aerosol and Air Quality Research*, 16,  
464 885-899, 10.4209/aaqr.2015.06.0391, 2016.

465 Christner, B. C., Morris, C. E., Foreman, C. M., Cai, R. M., and Sands, D. C.: Ubiquity of biological ice nucleators in snowfall,  
466 *Science*, 319, 1214-1214, 10.1126/science.1149757, 2008.

467 Collaud Coen, M., Weingartner, E., Schaub, D., Hueglin, C., Corrigan, C., Henning, S., Schwikowski, M., and Baltensperger, U.:  
468 Saharan dust events at the Jungfraujoch: detection by wavelength dependence of the single scattering albedo and first  
469 climatology analysis, *Atmos. Chem. Phys.*, 4, 2465-2480, 2004.

470 Collaud Coen, M., Weingartner, E., Furger, M., Nyeki, S., Prevot, A. S. H., Steinbacher, M., and Baltensperger, U.: Aerosol  
471 climatology and planetary boundary influence at the Jungfraujoch analyzed by synoptic weather types, *Atmos Chem Phys*,  
472 11, 5931-5944, 10.5194/acp-11-5931-2011, 2011.

473 Collaud Coen, M., Andrews, E., Aliaga, D., Andrade, M., Angelov, H., Bukowiecki, N., Ealo, M., Fialho, P., Flentje, H., Hallar,  
474 A. G., Hooda, R., Kalapov, I., Krejci, R., Lin, N.-H., Marinoni, A., Ming, J., Nguyen, N. A., Pandolfi, M., Pont, V., Ries,  
475 L., Rodriguez, S., Schauer, G., Sellegri, K., Sharma, S., Sun, J., Tunved, P., Velasquez, P., and Ruffieux, D.: Identification  
476 of topographic features influencing aerosol observations at high altitude stations, *Atmos. Chem. Phys.*, 18, 12289-12313,  
477 2018.

478 Coluzza, I., Creamean, J., Rossi, M., Wex, H., Alpert, P., Bianco, V., Boose, Y., Dellago, C., Felgitsch, L., Fröhlich-Nowoisky,  
479 J., Herrmann, H., Jungblut, S., Kanji, Z., Menzl, G., Moffett, B., Moritz, C., Mutzel, A., Pöschl, U., Schauperl, M., Scheel,  
480 J., Stopelli, E., Stratmann, F., Grothe, H., and Schmale, D.: Perspectives on the Future of Ice Nucleation Research:  
481 Research Needs and Unanswered Questions Identified from Two International Workshops, *Atmosphere*, 8, 138, 2017.

482 Conen, F., Morris, C. E., Leifeld, J., Yakutin, M. V., and Alewell, C.: Biological residues define the ice nucleation properties of  
483 soil dust, *Atmos. Chem. Phys.*, 11, 9643-9648, 10.5194/acp-11-9643-2011, 2011.

484 Conen, F., Rodriguez, S., Huglin, C., Henne, S., Herrmann, E., Bukowiecki, N., and Alewell, C.: Atmospheric ice nuclei at the  
485 high-altitude observatory Jungfraujoch, Switzerland, *Tellus B*, 67, 10.3402/tellusb.v67.25014, 2015.

486 Conen, F., and Yakutin, M. V.: Soils rich in biological ice-nucleating particles abound in ice-nucleating macromolecules likely  
487 produced by fungi, *Biogeosciences*, 15, 4381-4385, 10.5194/bg-15-4381-2018, 2018.

488 Creamean, J. M., Suski, K. J., Rosenfeld, D., Cazorla, A., DeMott, P. J., Sullivan, R. C., White, A. B., Ralph, F. M., Minnis, P.,  
489 Comstock, J. M., Tomlinson, J. M., and Prather, K. A.: Dust and Biological Aerosols from the Sahara and Asia Influence  
490 Precipitation in the Western U.S., *Science*, 339, 1572-1578, DOI 10.1126/science.1227279, 2013.

491 Creamean, J. M., Kirpes, R. M., Pratt, K. A., Spada, N. S., Maahn, M., de Boer, G., Schnell, R. C., and China, S.: Marine and  
492 terrestrial influences on ice nucleating particles during continuous springtime measurements in an Arctic oilfield location,  
493 *Atmos Chem Phys*, 18, 1-20, <https://doi.org/10.5194/acp-18-1-2018>, 2018a.

494 Creamean, J. M., Primm, K. M., Tolbert, M. A., Hall, E. G., Wendell, J., Jordan, A., Sheridan, P. J., Smith, J., and Schnell, R. C.:  
495 HOVERCAT: A novel aerial system for evaluation of aerosol-cloud interactions, *Atmos. Meas. Tech.*, submitted, 2018b.

496 Cziczco, D. J., Ladino, L., Boose, Y., Kanji, Z. A., Kupiszewski, P., Lance, S., Mertes, S., and Wex, H.: Measurements of Ice  
497 Nucleating Particles and Ice Residuals, *Meteorological Monographs*, 58, 8.1-8.13, 10.1175/amsmonographs-d-16-0008.1,  
498 2017.

499 DeMott, P. J., Chen, Y., Kreidenweis, S. M., Rogers, D. C., and Sherman, D. E.: Ice formation by black carbon particles, *Geophys*  
500 *Res Lett*, 26, 2429-2432, Doi 10.1029/1999gl900580, 1999.

501 DeMott, P. J., Prenni, A. J., Liu, X., Kreidenweis, S. M., Petters, M. D., Twohy, C. H., Richardson, M. S., Eidhammer, T., and  
502 Rogers, D. C.: Predicting global atmospheric ice nuclei distributions and their impacts on climate, *P Natl Acad Sci USA*,  
503 107, 11217-11222, 10.1073/pnas.0910818107, 2010.

504 DeMott, P. J., Hill, T. C. J., McCluskey, C. S., Prather, K. A., Collins, D. B., Sullivan, R. C., Ruppel, M. J., Mason, R. H., Irish,  
505 V. E., Lee, T., Hwang, C. Y., Rhee, T. S., Snider, J. R., McMeeking, G. R., Dhaniyala, S., Lewis, E. R., Wentzell, J. J.  
506 B., Abbatt, J., Lee, C., Sultana, C. M., Ault, A. P., Axson, J. L., Martinez, M. D., Venero, I., Santos-Figueroa, G., Stokes,  
507 M. D., Deane, G. B., Mayol-Bracero, O. L., Grassian, V. H., Bertram, T. H., Bertram, A. K., Moffett, B. F., and Franc,  
508 G. D.: Sea spray aerosol as a unique source of ice nucleating particles, *P Natl Acad Sci USA*, 113, 5797-5803,  
509 10.1073/pnas.1514034112, 2016.

510 DeMott, P. J., Möhler, O., Cziczco, D. J., Hiranuma, N., Petters, M. D., Petters, S. S., Belosi, F., Bingemer, H. G., Brooks, S. D.,  
511 Budke, C., Burkert-Kohn, M., Collier, K. N., Danielczok, A., Eppers, O., Felgitsch, L., Garimella, S., Grothe, H., Herenz,  
512 P., Hill, T. C. J., Höhler, K., Kanji, Z. A., Kiselev, A., Koop, T., Kristensen, T. B., Krüger, K., Kulkarni, G., Levin, E. J.  
513 T., Murray, B. J., Nicosia, A., D., O. S., A., P., J., P. M., C., P. H., Reicher, N., Rothenberg, D. A., Rudich, Y., Santachiara,  
514 G., Schiebel, T., Schrod, J., Seifried, T. M., Stratmann, F., Sullivan, R. C., Suski, K. J., Szakáll, M., Taylor, H. P., Ullrich,  
515 R., Vergara-Temprado, J., Wagner, R., Whale, T. F., Weber, D., Welti, A., Wilson, T. W., Wolf, M. J., and Zenker, J.:  
516 The Fifth International Workshop on Ice Nucleation phase 2 (FIN-02): Laboratory intercomparison of ice nucleation  
517 measurements, *Atmos. Meas. Tech.*, in review, <https://doi.org/10.5194/amt-2018-191>, 2018.

518 Despres, V. R., Huffman, J. A., Burrows, S. M., Hoose, C., Safatov, A. S., Buryak, G., Frohlich-Nowoisky, J., Elbert, W., Andreae,  
519 M. O., Poschl, U., and Jaenicke, R.: Primary biological aerosol particles in the atmosphere: a review, *Tellus B*, 64,  
520 10.3402/tellusb.v64i0.15598, 2012.

521 Draxler, R. R.: HYSPLIT4 user's guide, NOAA Air Resources Laboratory, Silver Spring, MD., 1999.

522 Draxler, R. R., and Rolph, G.: HYSPLIT (HYbrid Single-Particle Lagrangian Integrated Trajectory) Model access via NOAA ARL  
523 READY website (<http://ready.arl.noaa.gov/hysplit.php>), NOAA Air Resources Laboratory, Silver Spring, MD, 2011.

524 Eriksen Hammer, S., Mertes, S., Schneider, J., Ebert, M., Kandler, K., and Weinbruch, S.: Composition of ice particle residuals in  
525 mixed-phase clouds at Jungfraujoch (Switzerland): enrichment and depletion of particle groups relative to total aerosol,  
526 *Atmos. Chem. Phys.*, 18, 13987-14003, 2018.

527 Fridlind, A. M., Diedenhoven, B. v., Ackerman, A. S., Avramov, A., Mrowiec, A., Morrison, H., Zuidema, P., and Shupe, M. D.:  
528 A FIRE-ACE/SHEBA Case Study of Mixed-Phase Arctic Boundary Layer Clouds: Entrainment Rate Limitations on  
529 Rapid Primary Ice Nucleation Processes, *Journal of the Atmospheric Sciences*, 69, 365-389, 10.1175/jas-d-11-052.1,  
530 2012.

531 Frohlich-Nowoisky, J., Burrows, S. M., Xie, Z., Engling, G., Solomon, P. A., Fraser, M. P., Mayol-Bracero, O. L., Artaxo, P.,  
532 Begerow, D., Conrad, R., Andreae, M. O., Despres, V. R., and Poschl, U.: Biogeography in the air: fungal diversity over  
533 land and oceans, *Biogeosciences*, 9, 1125-1136, 10.5194/bg-9-1125-2012, 2012.

534 Frohlich-Nowoisky, J., Kampf, C. J., Weber, B., Huffman, J. A., Pohlker, C., Andreae, M. O., Lang-Yona, N., Burrows, S. M.,  
535 Gunthe, S. S., Elbert, W., Su, H., Hoor, P., Thines, E., Hoffmann, T., Despres, V. R., and Poschl, U.: Bioaerosols in the  
536 Earth system: Climate, health, and ecosystem interactions, *Atmos Res*, 182, 346-376, 10.1016/j.atmosres.2016.07.018,  
537 2016.

538 Fröhlich-Nowoisky, J., Hill, T. C. J., Pummer, B. G., Yordanova, P., Franc, G. D., and Pöschl, U.: Ice nucleation activity in the  
539 widespread soil fungus *Mortierella alpina*, *Biogeosciences*, 12, 1057-1071, 10.5194/bg-12-1057-2015, 2015.

540 Ganguly, M., Dib, S., and Ariya, P. A.: Purely Inorganic Highly Efficient Ice Nucleating Particle, *ACS Omega*, 3, 3384-3395,  
541 10.1021/acsomega.7b01830, 2018.

542 Griffiths, A. D., Conen, F., Weingartner, E., Zimmermann, L., Chambers, S. D., Williams, A. G., and Steinbacher, M.: Surface-  
543 to-mountaintop transport characterised by radon observations at the Jungfraujoch, *Atmos Chem Phys*, 14, 12763-12779,  
544 10.5194/acp-14-12763-2014, 2014.

545 Hader, J. D., Wright, T. P., and Petters, M. D.: Contribution of pollen to atmospheric ice nuclei concentrations, *Atmos. Chem.*  
546 *Phys.*, 14, 5433-5449, 10.5194/acp-14-5433-2014, 2014a.

547 Hader, J. D., Wright, T. P., and Petters, M. D.: Contribution of pollen to atmospheric ice nuclei concentrations, *Atmos Chem Phys*,  
548 14, 5433-5449, 10.5194/acp-14-5433-2014, 2014b.

549 Hara, K., Maki, T., Kakikawa, M., Kobayashi, F., and Matsuki, A.: Effects of different temperature treatments on biological ice  
550 nuclei in snow samples, *Atmos Environ*, 140, 415-419, 10.1016/j.atmosenv.2016.06.011, 2016.

551 Herrmann, E., Weingartner, E., Henne, S., Vuilleumier, L., Bukowiecki, N., Steinbacher, M., Conen, F., Coen, M. C., Hammer,  
552 E., Juranyi, Z., Baltensperger, U., and Gysel, M.: Analysis of long-term aerosol size distribution data from Jungfraujoch  
553 with emphasis on free tropospheric conditions, cloud influence, and air mass transport, *J Geophys Res-Atmos*, 120, 9459-  
554 9480, 10.1002/2015jd023660, 2015.

555 Hill, T. C. J., DeMott, P. J., Tobo, Y., Fröhlich-Nowoisky, J., Moffett, B. F., Franc, G. D., and Kreidenweis, S. M.: Sources of  
556 organic ice nucleating particles in soils, *Atmos. Chem. Phys.*, 16, 7195-7211, 10.5194/acp-16-7195-2016, 2016.

557 Hoose, C., and Möhler, O.: Heterogeneous ice nucleation on atmospheric aerosols: a review of results from laboratory experiments,  
558 *Atmos. Chem. Phys.*, 12, 9817-9854, 10.5194/acp-12-9817-2012, 2012.

559 Hu, W., Niu, H. Y., Murata, K., Wu, Z. J., Hu, M., Kojima, T., and Zhang, D. Z.: Bacteria in atmospheric waters: Detection,  
560 characteristics and implications, *Atmos Environ*, 179, 201-221, 10.1016/j.atmosenv.2018.02.026, 2018.

561 Hummel, M., Hoose, C., Gallagher, M., Healy, D. A., Huffman, J. A., O'Connor, D., Poschl, U., Pohlker, C., Robinson, N. H.,  
562 Schnaiter, M., Sodeau, J. R., Stengel, M., Toprak, E., and Vogel, H.: Regional-scale simulations of fungal spore aerosols  
563 using an emission parameterization adapted to local measurements of fluorescent biological aerosol particles, *Atmos*  
564 *Chem Phys*, 15, 6127-6146, 10.5194/acp-15-6127-2015, 2015.

565 Jaenicke, R.: Atmospheric aerosols and global climate, *Journal of Aerosol Science*, 11, 577-588, [https://doi.org/10.1016/0021-](https://doi.org/10.1016/0021-8502(80)90131-7)  
566 [8502\(80\)90131-7](https://doi.org/10.1016/0021-8502(80)90131-7), 1980.

567 Jaenicke, R.: Abundance of Cellular Material and Proteins in the Atmosphere, *Science*, 308, 73-73, 10.1126/science.1106335,  
568 2005.

569 Jaenicke, R., Matthias-Maser, S., and Gruber, S.: Omnipresence of biological material in the atmosphere, *Environmental*  
570 *Chemistry*, 4, 217-220, <https://doi.org/10.1071/EN07021>, 2007.

571 Kanji, Z. A., Ladino, L. A., Wex, H., Boose, Y., Burkert-Kohn, M., Cziczo, D. J., and Krämer, M.: Overview of Ice Nucleating  
572 Particles, *Meteorological Monographs*, 58, 1.1-1.33, 10.1175/amsmonographs-d-16-0006.1, 2017.

573 Kellogg, C. A., and Griffin, D. W.: Aerobiology and the global transport of desert dust, *Trends Ecol Evol*, 21, 638-644,  
574 10.1016/j.tree.2006.07.004, 2006.

575 Kieft, T. L.: Ice Nucleation Activity in Lichens, *Applied and Environmental Microbiology*, 54, 1678-1681, 1988.

576 Knopf, D. A., Alpert, P. A., Wang, B., and Aller, J. Y.: Stimulation of ice nucleation by marine diatoms, *Nature Geoscience*, 4,  
577 88, 10.1038/ngeo1037, 2010.

578 Korolev, A., McFarquhar, G., Field, P. R., Franklin, C., Lawson, P., Wang, Z., Williams, E., Abel, S. J., Axisa, D., Borrmann, S.,  
579 Crosier, J., Fugal, J., Krämer, M., Lohmann, U., Schlenzcek, O., Schnaiter, M., and Wendisch, M.: Mixed-Phase Clouds:  
580 Progress and Challenges, *Meteorological Monographs*, 58, 5.1-5.50, 10.1175/amsmonographs-d-17-0001.1, 2017.

581 Lacher, L., Lohmann, U., Boose, Y., Zipori, A., Herrmann, E., Bukowiecki, N., Steinbacher, M., and Kanji, Z. A.: The Horizontal  
582 Ice Nucleation Chamber (HINC): INP measurements at conditions relevant for mixed-phase clouds at the High Altitude  
583 Research Station Jungfraujoch, *Atmos. Chem. Phys.*, 17, 15199–15224, <https://doi.org/10.5194/acp-17-15199-2017>,  
584 2017.

585 Lacher, L., DeMott, P. J., Levin, E. J. T., Suski, K. J., Boose, Y., Zipori, A., Herrmann, E., Bukowiecki, N., Steinbacher, M., Gute,  
586 E., Abbatt, J. P. D., Lohmann, U., and Kanji, Z. A.: Background Free-Tropospheric Ice Nucleating Particle Concentrations  
587 at Mixed-Phase Cloud Conditions, *Journal of Geophysical Research: Atmospheres*, 123, doi:10.1029/2018JD028338,  
588 2018a.

589 Lacher, L., Steinbacher, M., Bukowiecki, N., Herrmann, E., Zipori, A., and Kanji, Z. A.: Impact of Air Mass Conditions and  
590 Aerosol Properties on Ice Nucleating Particle Concentrations at the High Altitude Research Station Jungfraujoch,  
591 *Atmosphere*, 9, 2018b.

592 Langham, E. J., and Mason, B. J.: The Heterogeneous and Homogeneous Nucleation of Supercooled Water, *Proc R Soc Lon Ser-*  
593 *A*, 247, 493-&, DOI 10.1098/rspa.1958.0207, 1958.

594 Lloyd, G., Choulaton, T. W., Bower, K. N., Gallagher, M. W., Connolly, P. J., Flynn, M., Farrington, R., Crosier, J., Schlenzcek,  
595 O., Fugal, J., and Henneberger, J.: The origins of ice crystals measured in mixed-phase clouds at the high-alpine site  
596 Jungfraujoch, *Atmos Chem Phys*, 15, 12953-12969, 10.5194/acp-15-12953-2015, 2015.

597 Lohmann, U., Henneberger, J., Henneberg, O., Fugal, J. P., Bühl, J., and Kanji, Z. A.: Persistence of orographic mixed-phase  
598 clouds, *Geophys Res Lett*, 43, 512-510,519, doi:10.1002/2016GL071036, 2016.

599 Mason, R. H., Si, M., Chou, C., Irish, V. E., Dickie, R., Elizondo, P., Wong, R., Brintnell, M., Elsasser, M., Lassar, W. M., Pierce,  
600 K. M., Leitch, W. R., MacDonald, A. M., Platt, A., Toom-Sauntry, D., Sarda-Estevé, R., Schiller, C. L., Suski, K. J.,  
601 Hill, T. C. J., Abbatt, J. P. D., Huffman, J. A., DeMott, P. J., and Bertram, A. K.: Size-resolved measurements of ice-  
602 nucleating particles at six locations in North America and one in Europe, *Atmos Chem Phys*, 16, 1637-1651, 10.5194/acp-  
603 16-1637-2016, 2016.

604 McCluskey, C. S., Hill, T. C. J., Malfatti, F., Sultana, C. M., Lee, C., Santander, M. V., Beall, C. M., Moore, K. A., Cornwell, G.  
605 C., Collins, D. B., Prather, K. A., Jayarathne, T., Stone, E. A., Azam, F., Kreidenweis, S. M., and DeMott, P. J.: A  
606 Dynamic Link between Ice Nucleating Particles Released in Nascent Sea Spray Aerosol and Oceanic Biological Activity  
607 during Two Mesocosm Experiments, *Journal of the Atmospheric Sciences*, 74, 151-166, 10.1175/Jas-D-16-0087.1, 2017.

608 Mignani, C., Creamean, J. M., Zimmermann, L., Alewell, C., and Conen, F.: Direct evidence for secondary ice formation at around  
609 -15 °C in mixed-phase clouds, *Atmos. Chem. Phys. Discuss.*, under review, 2018.

610 Morris, C. E., Georgakopoulos, D. G., and Sands, D. C.: Ice nucleation active bacteria and their potential role in precipitation, *J*  
611 *Phys Iv*, 121, 87-103, DOI 10.1051/jp4:2004121004, 2004.

612 Morris, C. E., Sands, D. C., Bardin, M., Jaenicke, R., Vogel, B., Leyronas, C., Ariya, P. A., and Psenner, R.: Microbiology and  
613 atmospheric processes: research challenges concerning the impact of airborne micro-organisms on the atmosphere and  
614 climate, *Biogeosciences*, 8, 17-25, 10.5194/bg-8-17-2011, 2011.

615 Morris, C. E., Conen, F., Huffman, J. A., Phillips, V., Poschl, U., and Sands, D. C.: Bioprecipitation: a feedback cycle linking  
616 Earth history, ecosystem dynamics and land use through biological ice nucleators in the atmosphere, *Global Change Biol*,  
617 20, 341-351, 10.1111/gcb.12447, 2014.

618 Morris, C. E., Soubeyrand, S., Bigg, E. K., Creamean, J. M., and Sands, D. C.: Mapping Rainfall Feedback to Reveal the Potential  
619 Sensitivity of Precipitation to Biological Aerosols, *Bulletin of the American Meteorological Society*, 98, 1109-1118,  
620 <https://doi.org/10.1175/BAMS-D-15-00293.1>, 2017.

621 Mossop, S. C., and Thorndike, N. S. C.: The Use of Membrane Filters in Measurements of Ice Nucleus Concentration. I. Effect of  
622 Sampled Air Volume, *Journal of Applied Meteorology*, 5, 474-480, 10.1175/1520-  
623 0450(1966)005<0474:tuomfi>2.0.co;2, 1966.

624 Murray, B. J., O'Sullivan, D., Atkinson, J. D., and Webb, M. E.: Ice nucleation by particles immersed in supercooled cloud droplets,  
625 *Chem Soc Rev*, 41, 6519-6554, Doi 10.1039/C2cs35200a, 2012.

626 O'Sullivan, D., Murray, B. J., Malkin, T. L., Whale, T. F., Umo, N. S., Atkinson, J. D., Price, H. C., Baustian, K. J., Browse, J.,  
627 and Webb, M. E.: Ice nucleation by fertile soil dusts: relative importance of mineral and biogenic components, *Atmos.*  
628 *Chem. Phys.*, 14, 1853-1867, 10.5194/acp-14-1853-2014, 2014.

629 O'Sullivan, D., Murray, B. J., Ross, J. F., and Webb, M. E.: The adsorption of fungal ice-nucleating proteins on mineral dusts: a  
630 terrestrial reservoir of atmospheric ice-nucleating particles, *Atmos Chem Phys*, 16, 7879-7887, 10.5194/acp-16-7879-  
631 2016, 2016.

632 Petters, M. D., and Wright, T. P.: Revisiting ice nucleation from precipitation samples, *Geophys Res Lett*, 42, 8758-8766,  
633 10.1002/2015gl065733, 2015.

634 Price, H. C., Baustian, K. J., McQuaid, J. B., Blyth, A., Bower, K. N., Choulaton, T., Cotton, R. J., Cui, Z., Field, P. R., Gallagher,  
635 M., Hawker, R., Merrington, A., Miltenberger, A., Neely, R. R., Parker, S. T., Rosenberg, P. D., Taylor, J. W., Trembath,  
636 J., Vergara-Temprado, J., Whale, T. F., Wilson, T. W., Young, G., and Murray, B. J.: Atmospheric Ice-Nucleating  
637 Particles in the Dusty Tropical Atlantic, *J Geophys Res-Atmos*, 123, 2175-2193, 10.1002/2017jd027560, 2018.

638 Reche, I., D'Orta, G., Mladenov, N., Winget, D. M., and Suttle, C. A.: Deposition rates of viruses and bacteria above the  
639 atmospheric boundary layer, *Isme J*, 12, 1154-1162, 10.1038/s41396-017-0042-4, 2018.

640 Sahyoun, M., Korsholm, U. S., Sorensen, J. H., Santl-Temkiv, T., Finster, K., Gosewinkel, U., and Nielsen, N. W.: Impact of  
641 bacterial ice nucleating particles on weather predicted by a numerical weather prediction model, *Atmos Environ*, 170, 33-  
642 44, 10.1016/j.atmosenv.2017.09.029, 2017.

643 Schnell, R. C., and Vali, G.: Biogenic Ice Nuclei .1. Terrestrial and Marine Sources, *Journal of the Atmospheric Sciences*, 33,  
644 1554-1564, Doi 10.1175/1520-0469(1976)033<1554:Binpit>2.0.Co;2, 1976.

645 Stein, A. F., Draxler, R. R., Rolph, G. D., Stunder, B. J. B., Cohen, M. D., and Ngan, F.: NOAA's HYSPLIT Atmospheric Transport  
646 and Dispersion Modeling System, *Bulletin of the American Meteorological Society*, 96, 2059-2077, 10.1175/bams-d-14-  
647 00110.1, 2015.

648 Stopelli, E., Conen, F., Zimmermann, L., Alewell, C., and Morris, C. E.: Freezing nucleation apparatus puts new slant on study of  
649 biological ice nucleators in precipitation, *Atmos Meas Tech*, 7, 129-134, 10.5194/amt-7-129-2014, 2014.

650 Stopelli, E., Conen, F., Morris, C. E., Herrmann, E., Bukowiecki, N., and Alewell, C.: Ice nucleation active particles are efficiently  
651 removed by precipitating clouds, *Scientific Reports*, 5, 16433, 10.1038/srep16433, 2015.

652 Stopelli, E., Conen, F., Morris, C. E., Herrmann, E., Henne, S., Steinbacher, M., and Alewell, C.: Predicting abundance and  
653 variability of ice nucleating particles in precipitation at the high-altitude observatory Jungfraujoch, *Atmos Chem Phys*,  
654 16, 8341-8351, 10.5194/acp-16-8341-2016, 2016.

655 Stopelli, E., Conen, F., Guilbaud, C., Zopfi, J., Alewell, C., and Morris, C. E.: Ice nucleators, bacterial cells and *Pseudomonas*  
656 *syringae* in precipitation at Jungfraujoch, *Biogeosciences*, 14, 1189-1196, 10.5194/bg-14-1189-2017, 2017.

657 Storelmo, T., Hoose, C., and Eriksson, P.: Global modeling of mixed-phase clouds: The albedo and lifetime effects of aerosols,  
658 *Journal of Geophysical Research: Atmospheres*, 116, doi:10.1029/2010JD014724, 2011.

659 Suski, K. J., Hill, T. C. J., Levin, E. J. T., Miller, A., DeMott, P. J., and Kreidenweis, S. M.: Agricultural harvesting emissions of  
660 ice-nucleating particles, *Atmos. Chem. Phys.*, 18, 13755-13771, 2018.

661 Tesson, S. V. M., Skjøth, C. A., Šantl-Temkiv, T., and Löndahl, J.: Airborne Microalgae: Insights, Opportunities and Challenges,  
662 *Applied and Environmental Microbiology*, 10.1128/aem.03333-15, 2016.

663 Tobo, Y., DeMott, P. J., Hill, T. C. J., Prenni, A. J., Swoboda-Colberg, N. G., Franc, G. D., and Kreidenweis, S. M.: Organic matter  
664 matters for ice nuclei of agricultural soil origin, *Atmos. Chem. Phys.*, 14, 8521-8531, 10.5194/acp-14-8521-2014, 2014.

665 Tobo, Y.: An improved approach for measuring immersion freezing in large droplets over a wide temperature range, *Scientific*  
666 *Reports*, 6, ARTN 3293010.1038/srep32930, 2016.

667 Twohy, C. H., McMeeking, G. R., DeMott, P. J., McCluskey, C. S., Hill, T. C. J., Burrows, S. M., Kulkarni, G. R., Tanarhte, M.,  
668 Kafle, D. N., and Toohey, D. W.: Abundance of fluorescent biological aerosol particles at temperatures conducive to the  
669 formation of mixed-phase and cirrus clouds, *Atmos Chem Phys*, 16, 8205-8225, 10.5194/acp-16-8205-2016, 2016.

670 Twomey, S.: The Influence of Pollution on the Shortwave Albedo of Clouds, *Journal of the Atmospheric Sciences*, 34, 1149-1152,  
671 10.1175/1520-0469(1977)034<1149:tiopot>2.0.co;2, 1977.

672 Vali, G., and Stansbury, E. J.: Time-Dependent Characteristics of Heterogeneous Nucleation of Ice, *Can J Phys*, 44, 477-+, DOI  
673 10.1139/p66-044, 1966.

674 Vali, G.: Quantitative Evaluation of Experimental Results an the Heterogeneous Freezing Nucleation of Supercooled Liquids,  
675 *Journal of the Atmospheric Sciences*, 28, 402-409, 10.1175/1520-0469(1971)028<0402:qeoera>2.0.co;2, 1971.

676 Vali, G., Christensen, M., Fresh, R. W., Galyan, E. L., Maki, L. R., and Schnell, R. C.: Biogenic Ice Nuclei .2. Bacterial Sources,  
677 *Journal of the Atmospheric Sciences*, 33, 1565-1570, Doi 10.1175/1520-0469(1976)033<1565:Binpib>2.0.Co;2, 1976.

678 Vali, G., DeMott, P. J., Möhler, O., and Whale, T. F.: Technical Note: A proposal for ice nucleation terminology, *Atmos. Chem.*  
679 *Phys.*, 15, 10263-10270, 10.5194/acp-15-10263-2015, 2015.

680 Vali, G.: Revisiting the differential freezing nucleus spectra derived from drop freezing experiments; methods of calculation,  
681 applications and confidence limits, *Atmos. Meas. Tech. Discuss.*, 2018, 1-18, 10.5194/amt-2018-309, 2018.

682 von Blohn, N., Mitra, S. K., Diehl, K., and Borrmann, S.: The ice nucleating ability of pollen: Part III: New laboratory studies in  
683 immersion and contact freezing modes including more pollen types, *Atmos Res*, 78, 182-189,  
684 10.1016/j.atmosres.2005.03.008, 2005.

685 Weingartner, E., Nyeki, S., and Baltensperger, U.: Seasonal and diurnal variation of aerosol size distributions ( $10 < D < 750$  nm)  
686 at a high-alpine site (Jungfraujoch 3580 m asl), *J Geophys Res-Atmos*, 104, 26809-26820, Doi 10.1029/1999jd900170,  
687 1999.

688 Wex, H., Augustin-Bauditz, S., Boose, Y., Budke, C., Curtius, J., Diehl, K., Dreyer, A., Frank, F., Hartmann, S., Hiranuma, N.,  
689 Jantsch, E., Kanji, Z. A., Kiselev, A., Koop, T., Mohler, O., Niedermeier, D., Nillius, B., Rosch, M., Rose, D., Schmidt,  
690 C., Steinke, I., and Stratmann, F.: Intercomparing different devices for the investigation of ice nucleating particles using  
691 Snomax (R) as test substance, *Atmos Chem Phys*, 15, 1463-1485, 10.5194/acp-15-1463-2015, 2015.

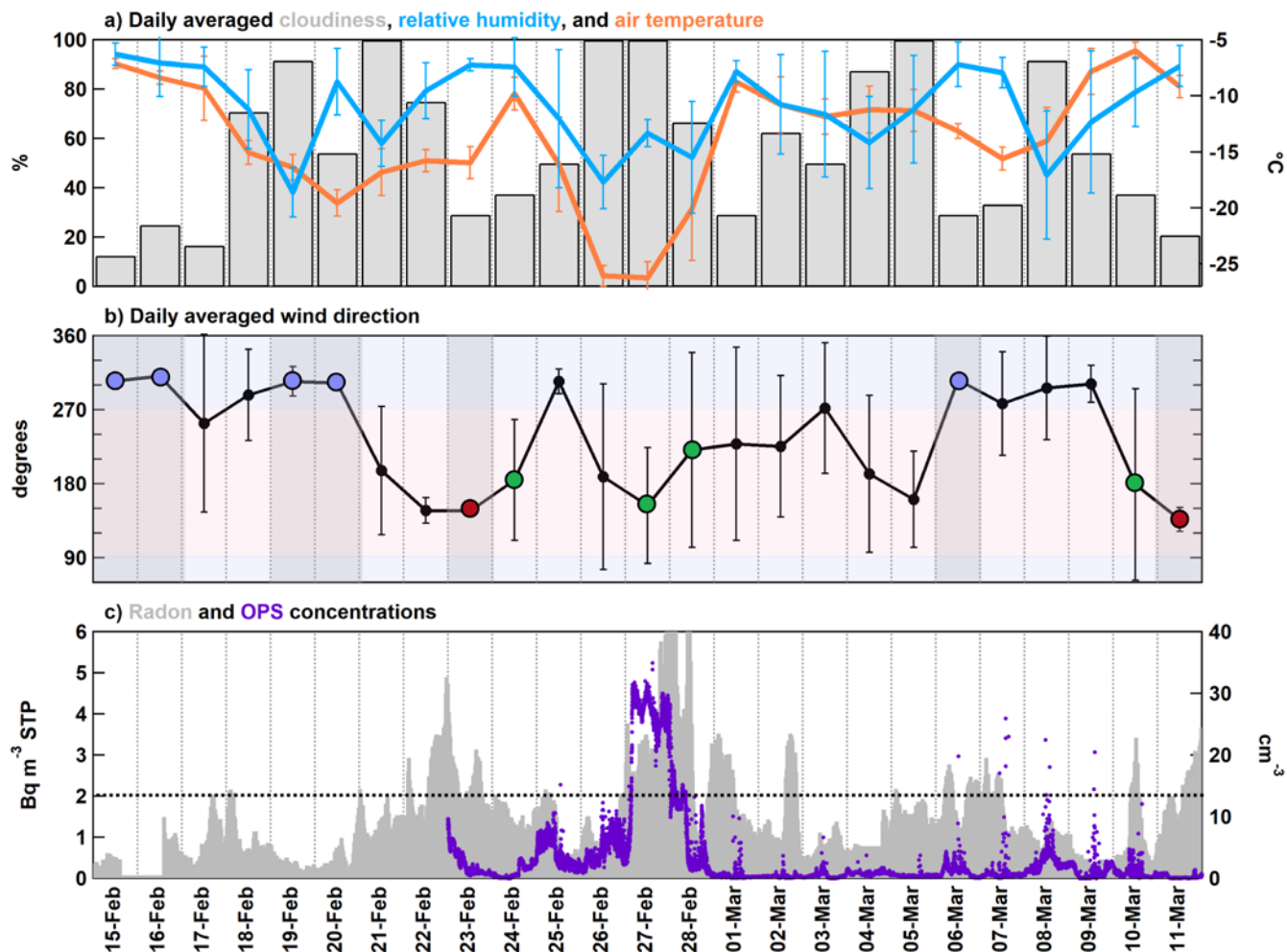
692 Wilson, T. W., Ladino, L. A., Alpert, P. A., Breckels, M. N., Brooks, I. M., Browse, J., Burrows, S. M., Carslaw, K. S., Huffman,  
693 J. A., Judd, C., Kilthau, W. P., Mason, R. H., McFiggans, G., Miller, L. A., Najera, J. J., Polishchuk, E., Rae, S., Schiller,  
694 C. L., Si, M., Temprado, J. V., Whale, T. F., Wong, J. P. S., Wurl, O., Yakobi-Hancock, J. D., Abbatt, J. P. D., Aller, J.  
695 Y., Bertram, A. K., Knopf, D. A., and Murray, B. J.: A marine biogenic source of atmospheric ice-nucleating particles,  
696 *Nature*, 525, 234-+, 10.1038/nature14986, 2015.

697 Wright, T. P., and Petters, M. D.: The role of time in heterogeneous freezing nucleation, *J Geophys Res-Atmos*, 118, 3731-3743,  
698 10.1002/jgrd.50365, 2013.  
699

700 **Table 1. Dates and times for cloud rime, snow, and aerosol samples collected during the 2018 winter INCAS study at Jungfraujoch. Also**  
 701 **shown are the dominant air mass sources (free troposphere or FT or boundary layer intrusion of BLI) for each day based on radon data.**  
 702 **Samples highlighted in blue and red are the northwest and southeast case studies, respectively. Samples highlighted in green represent**  
 703 **predominantly southerly days that were classified as Saharan dust events (SDEs) or BLI days.**

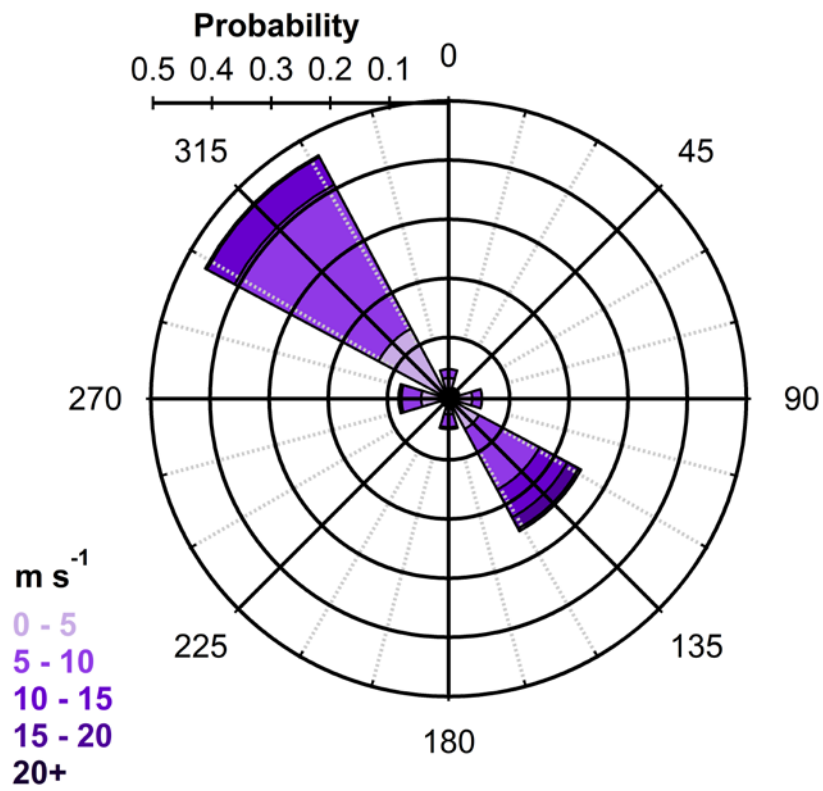
Date	Air mass	Cloud rime		Snow			Aerosol				
		Sample	Start (UTC)	Duration (hh:mm)	Sample	Start (UTC)	Duration (hh:mm)	Sample	Start (UTC)	Duration (hh:mm)	Stages
15-Feb	FT	Rime1	06:30	03:07	Snow1	07:15	01:15	DRUM1	10:00	12:00	A/B/C/D
		Rime2	09:37	02:13	Snow2	08:40	01:30	DRUM2	22:00	24:00	A/B/C/D
		Rime3	11:50	03:55	Snow3	10:10	01:35				
		Rime4	15:45	03:35	Snow4	12:45	02:30				
		Rime5	19:20	13:55	Snow5	15:20	04:00				
16-Feb	FT	Rime6	07:15	02:10	Snow6	07:15	02:02	DRUM3	22:00	24:00	A/B/C/D
		Rime7	09:29	02:41	Snow7	09:23	02:37				
					Snow8	14:00	17:50				
17-Feb	FT	Rime8	12:08	01:16	Snow9	07:50	02:23	DRUM4	22:00	24:00	A/B/C/D
		Rime9	13:24	02:23	Snow10	10:16	01:10				
		Rime10	15:47	03:12	Snow11	11:35	00:33				
		Rime11	18:59	06:48	Snow12	12:20	01:04				
					Snow13	13:42	01:00				
					Snow14	14:45	00:55				
					Snow15	15:54	02:54				
			Snow16	18:52	05:50						
18-Feb	FT	Rime12	00:47	08:22	None			DRUM5	22:00	24:00	A/B/C
19-Feb	FT	Rime13	21:00	10:50	Snow17	21:00	08:50	DRUM6	22:00	24:00	A/B/C
20-Feb	FT	Rime14	05:50	04:14	Snow18	05:50	04:14	DRUM7	22:00	24:00	A/B/C
		Rime15	12:08	02:17	Snow19	12:08	02:14				
21-Feb	FT	None		None			DRUM8	22:00	24:00	A/B/C/D	
22-Feb	BLI	None		None			DRUM9	22:00	24:00	A/B/C/D	
23-Feb	BLI	Rime16	20:00	14:30	Snow20	07:49	02:51	DRUM10	22:00	24:00	A/B/C/D
					Snow21	10:55	03:35				
					Snow22	14:40	02:42				
					Snow23	20:00	12:11				
24-Feb	FT, SDE	None		None			DRUM11	22:00	24:00	A/B/C	
25-Feb	FT	None		None			DRUM12	22:00	24:00	A/B	
26-Feb	FT	None		None			DRUM13	22:00	24:00	A/B/C	
27-Feb	BLI	None		None			DRUM14	22:00	24:00	A/B/C	
28-Feb	BLI	None		None			DRUM15	22:00	24:00	A/B/C	
01-Mar	BLI	None		None			DRUM16	22:00	24:00	A/B/C	
02-Mar	FT	None		None			DRUM17	22:00	24:00	A/B/C	
03-Mar	FT	None		None			DRUM18	22:00	24:00	A/B/C	
04-Mar	FT	None		None			DRUM19	22:00	24:00	A/B/C	
05-Mar	FT	Rime17	16:43	15:32	Snow24	21:52	08:16	DRUM20	22:00	24:00	A/B/C
06-Mar	BLI	Rime18	06:15	03:03	Snow25	06:15	02:50	DRUM21	22:00	24:00	A/B/C
		Rime19	09:18	05:42	Snow26	09:14	05:26				
		Rime20	15:00	02:08	Snow27	14:54	01:56				
		Rime21	17:08	04:41	Snow28	17:26	04:04				
		Rime22	22:38	21:40	Snow29	22:38	07:35				
07-Mar	BLI	Rime23	06:19	03:58	Snow30	06:19	01:19	DRUM22	22:00	24:00	A/B/C
		Rime24	10:17	05:40	Snow31	07:50	02:00				
		Rime25	15:57	08:31	Snow32	12:49	02:59				
		Rime26	22:28	06:34	Snow33	16:00	05:19				
					Snow34	22:28	06:27				
08-Mar	FT	None		None			DRUM23	22:00	24:00	A/B/C	
09-Mar	FT	None		None			DRUM24	22:00	24:00	A/B/C	
10-Mar	FT, SDE	Rime27	11:00	21:46	Snow35	06:00	04:00	DRUM25	22:00	24:00	A/B/C
					Snow36	10:10	01:56				
11-Mar	BLI	Rime28	06:46	02:59	Snow37	05:48	04:03	None			
		Rime29	09:56	03:49	Snow38	09:54	03:51				
		Rime30	13:45	04:48	Snow39	13:48	02:28				

704  
705



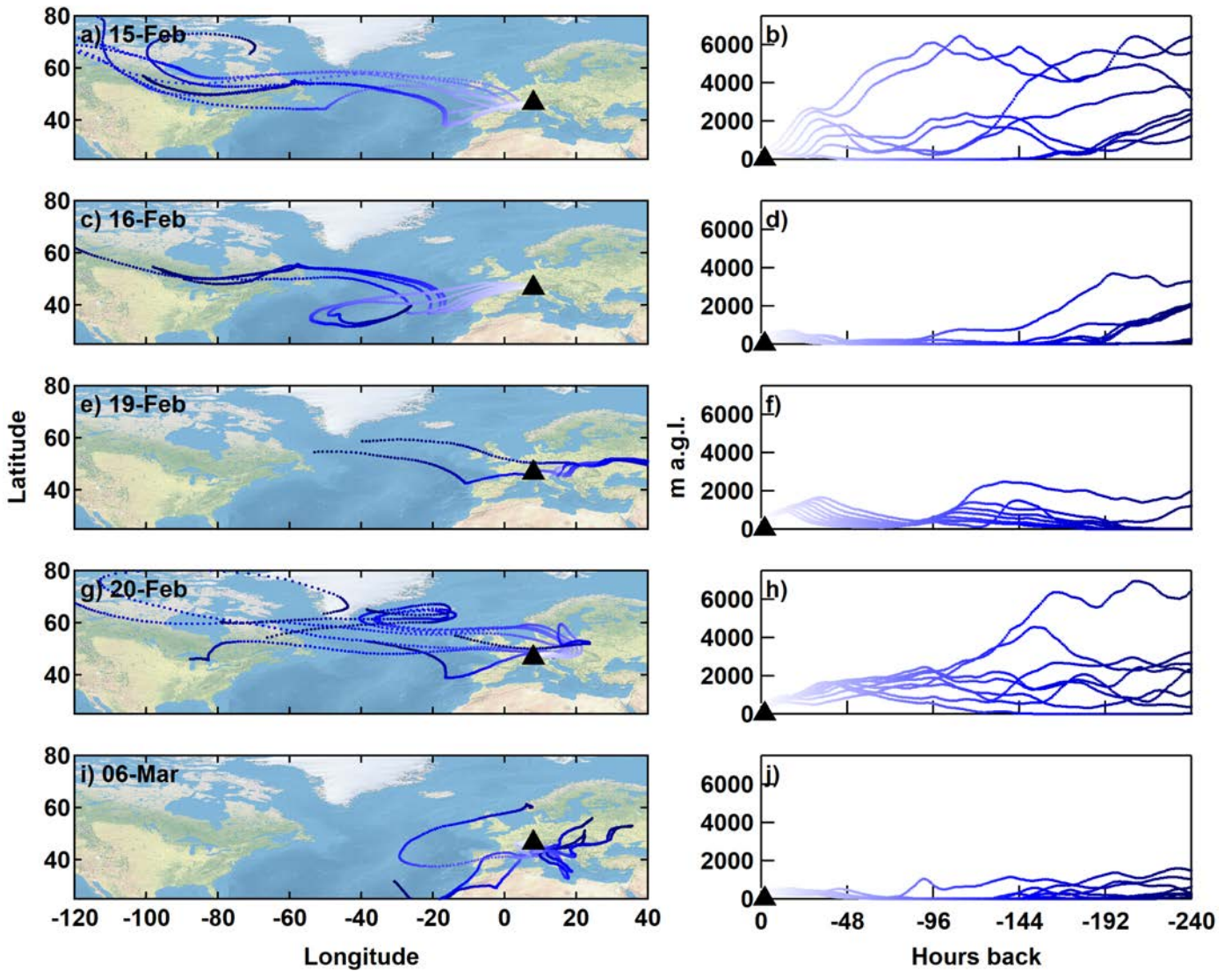
706  
707  
708  
709  
710  
711  
712  
713  
714

Figure 1. Daily averaged meteorological data at JFJ from INCAS, including a) percentage of cloudiness in the vertical profile over JFJ per the estimation by Herrmann et al. (2015), station relative humidity (%), and station air temperature (°C) and b) station wind direction. The background of b) is shaded horizontally by north (light blue) or south (light red) directions. Additionally, days with combined aerosol, cloud rime, and snow collections are vertically shaded grey. Blue and red markers for wind direction represent case study storm days that were entirely northwesterly or southeasterly, respectively. Green markers represent predominantly southerly days that were classified as Saharan dust events (SDEs) or heavy boundary layer influence days. c) Time series of radon (<sup>222</sup>Rn) corrected for standard temperature and pressure and OPS particle concentrations. The black dashed line indicates a threshold of 2 Bq m<sup>-3</sup> whereby boundary layer intrusion likely occurred at JFJ. OPS data were missing prior to 23 Feb. Error bars represent standard deviation.

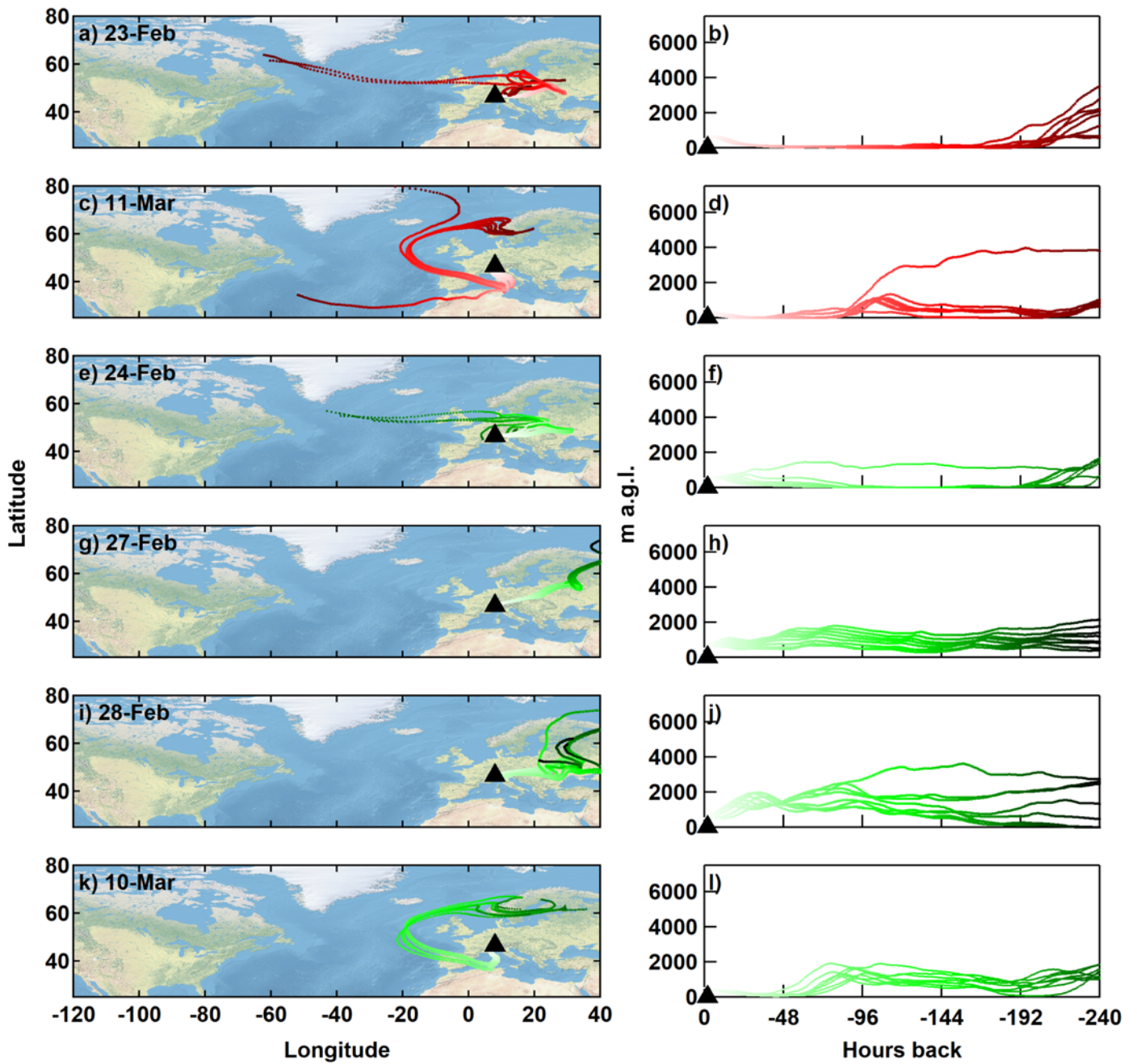


715  
716  
717

Figure 2. Rose plot for wind data during INCAS. Values correspond to wind direction binned by 45 degrees and wind speeds binned by 5 m s<sup>-1</sup>. The probability for wind speed to fall within these bins is plotted.

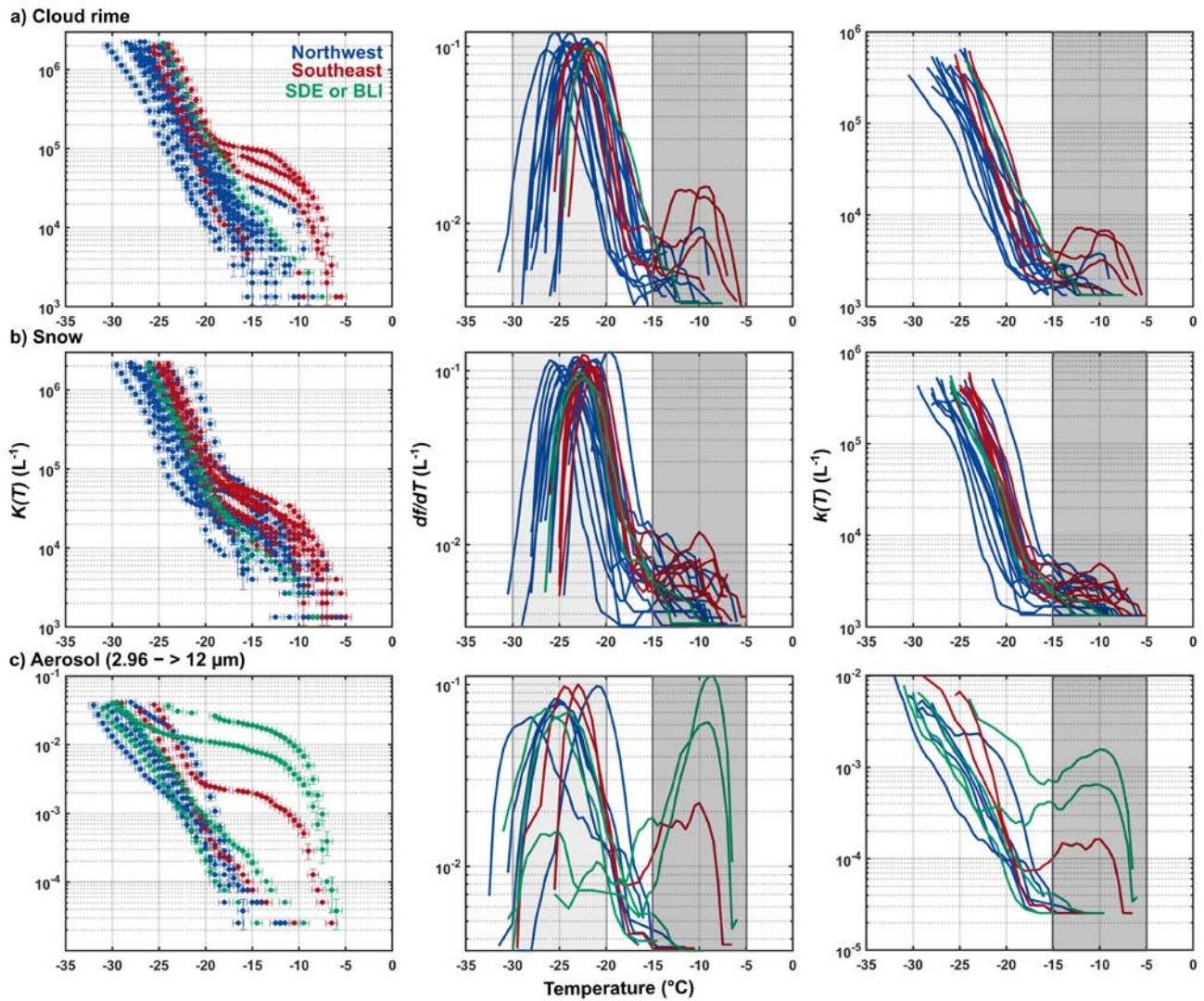


718  
 719 Figure 3. 10-day air mass backward trajectories initiated every 3 hours during sample collection for northwesterly case days ending at  
 720 500 m above ground level (a.g.l.). Trajectories are plotted by latitude-longitude (left) and altitude-time (right) profiles for 15 Feb (a, b),  
 721 16 Feb (c, d), 19 Feb (e, f), 20 Feb (g, h), and 06 Mar (i, j). Darker shades of blue represent trajectory points farther back in time.

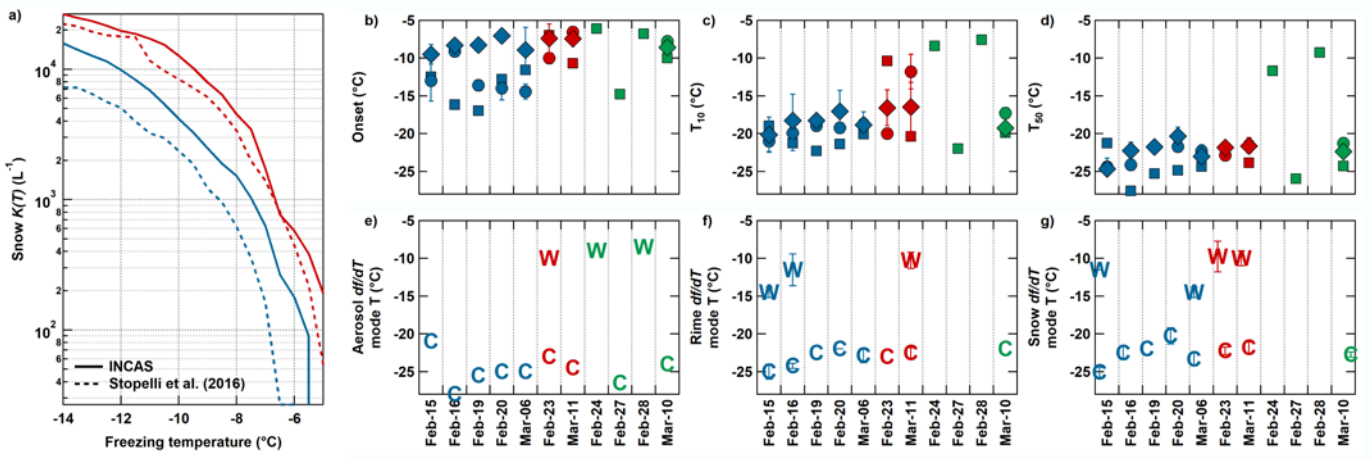


722  
723

Figure 4. Same as Figure 3, but for southeasterly (23 Feb and 11 Mar), SDE (24 Feb and 10 Mar), and BLI (27 and 28 Feb) case days.



724  
 725 Figure 5. Cumulative INP spectra ( $K(T)$ , on left), ~~normalized~~-differential of fraction frozen per temperature interval ( $df/dT$ ), and  
 726 ~~normalized~~-differential INP spectra ( $k(T)$ , on right) for the same samples of a) cloud rime, b) snow, and c) aerosol for the size range  $2.96 - > 12 \mu\text{m}$   
 727  $- > 12 \mu\text{m}$  in diameter. Spectra shown are for samples from the northwest (blue) and southeast (red) case study dates, in addition to SDE  
 728 and boundary layer intrusion (BLI) case days (green). Multiple cloud rime and snow samples were collected while one aerosol sample  
 729 from each size range was collected on northwest and southeast case study days (see Table 1). The warm mode region is indicated by the  
 730 dark grey shading in both the ~~normalized~~- $df/dT$  and  $k(T)$  spectra, while the cold mode region (for  $df/dT$  only) is shown in the ~~normalized~~  
 731  $df/dT$  spectra.



732  
 733 **Figure 6. a)** Comparison of INCAS cumulative snow INP concentrations for northwest (blue) and southeast (red) within the same range  
 734 of those reported by Stopelli et al. (2016) for measurements at JFJ during the 2012/13 winter season. Summary of INCAS INP  
 735 concentrations from aerosol (squares), cloud rime (circles), and snow samples (diamonds), including b) freezing onset temperatures, c)  
 736 the temperature in which 10% of drops froze, and d) the temperature in which 50% of the drops froze calculated from fraction frozen.  
 737 From the  $df/dT$  spectra, cold and warm mode temperatures are shown for e) aerosol, f) rime, and g) snow samples. The warm mode  
 738 temperatures from  $df/dT$  are the same as for  $k(T)$ . Blue, red, and green markers represent northwesterly cases, southeasterly cases, and  
 739 SDE and BLI case days, respectively. Some data points overlap and thus plots may appear to not have the same number of points per  
 740 sample.